

VAND-TH-98-02  
 DART-HEP-98/02  
 IF/UERJ-98/10  
 March 1998  
 hep-ph/9803394

## Strong Dissipative Behavior in Quantum Field Theory

Arjun Berera<sup>1 \*</sup>, Marcelo Gleiser<sup>2 †</sup> and Rudnei O. Ramos<sup>3 ‡</sup>

<sup>1</sup> *Department of Physics and Astronomy, Vanderbilt University,  
 Nashville, TN 37235, USA*

<sup>2</sup> *Department of Physics and Astronomy, Dartmouth College,  
 Hanover, NH 03755, USA,*

*Nasa/Fermilab Astrophysics Center, Fermi National Accelerator Laboratory  
 Batavia, IL 60510, USA,*

*Osservatorio Astronomico di Roma  
 Vialle del Parco Mellini 84, Roma I-00136, Italy*

<sup>3</sup> *Universidade do Estado do Rio de Janeiro, Inst. de Física - Depto. de Física Teórica,  
 20550-013 Rio de Janeiro, RJ, Brazil*

In Press Physical Review D, 1998

### Abstract

We study the conditions under which an overdamped regime can be attained in the dynamic evolution of a quantum field configuration. Using a

---

\*E-mail: berera@vuhep.phy.vanderbilt.edu

†E-mail: gleiser@peterpan.dartmouth.edu. NSF Presidential Faculty Fellow.

‡E-mail: rudnei@symbcomp.uerj.br

real-time formulation of finite temperature field theory, we compute the effective evolution equation of a scalar field configuration, quadratically interacting with a given set of other scalar fields. We then show that, in the overdamped regime, the dissipative kernel in the field equation of motion is closely related to the shear viscosity coefficient, as computed in scalar field theory at finite temperature. The effective dynamics is equivalent to a time-dependent Ginzburg-Landau description of the approach to equilibrium in phenomenological theories of phase transitions. Applications of our results, including a recently proposed inflationary scenario called “warm inflation”, are discussed.

PACS number(s): 98.80 Cq, 05.70.Ln, 11.10.Wx

## I. INTRODUCTION

Kinetic equations describe the time evolution of a certain chosen set of physical variables. The choice of physical variables in principle is arbitrary, but often in practice is governed by the measurement of interest. Typical examples are the order parameter of a complex system or the coordinate of a Brownian particle in a heat reservoir. The kinetic approach is usually implemented through a proper separation of the microscopic equations of motion of the chosen physical variables into regular and random parts. An averaging over the random part then generates the effective partition function for the regular part. This averaging is often referred to as a coarse-graining.

One typical application of the kinetic approach is when the physical variables of interest possess energy in relative excess or deficiency to the rest of a large system. Kinetic theory then describes the approach to equilibrium of the chosen physical variables, as for example in the kinetics of phase transitions or in Brownian motion. In the former case, the system is able to release energy to the environment due to some change in its internal state. Provided the environment is disproportionately large relative to the system, the process is irreversible. For a continuous transition, the focus of the present work, this process of equilibration can be

described by the monotonic change of an appropriate order parameter, which is the chosen physical variable. Many systems are known to relax in this manner. Phenomenologically, they are successfully described by the time-dependent Ginzburg-Landau theory [1].

Here we are interested in examining under which circumstances physical variables whose microscopic dynamics is second order in time, as for example the Higgs order parameter of spontaneous symmetry breaking, may have a dynamics which is effectively first order in time as in Ginzburg-Landau phenomenological models.

Qualitatively it is not difficult to argue the plausibility of this standard picture for the Higgs symmetry breaking scenario. A single variable, the Higgs order parameter, is modeled to control the release of energy to all the modes that couple to it. By basic notions of equipartition, one anticipates that some portion of the order parameter's energy will flow irreversibly to any given mode. Provided the Higgs order parameter couples to a sufficient number of modes, the motion of the order parameter will be overdamped.

In particle physics models, Higgs symmetry breaking is accompanied by mass generation. Thus the natural couplings for the Higgs field  $\phi$  to bosonic fields  $\chi_i$  is  $\phi^2\chi_i^2$ , gauge fields  $A_i^\mu$  is  $\phi^2 A^{i\mu} A_{i\mu}$  and fermionic fields  $\psi_i$  is  $\phi\bar{\psi}_i\psi_i$ . For a microscopic realization of time dependent Ginzburg-Landau theory for the Higgs scalar order parameter in a particle physics setting, these are the most obvious types of couplings to investigate. In this paper we will examine the case of purely bosonic couplings in the “symmetry restored” regime. That is, we will study the relaxation of an order parameter which is initially away from the only minimum of the free energy density describing the system. Much of the formalism required for this has already been done in [2] but we will extend that calculation to the overdamped regime. In an upcoming paper, we plan to study the symmetry broken case.

To our knowledge, this paper is the first study of overdamping in quantum field theory with realistic couplings between system and environment, as inspired by particle physics. Overdamping has been studied in quantum mechanical reaction rate theory for a particle escaping from a metastable state (for a review please see [3]). This is sometimes referred to as the Kramer's problem, with the overdamped limit also called the Smoluchowski limit.

Quantum mechanical models describing this problem are commonly of the system-heat bath type. Microscopic quantum mechanical models have been constructed along these lines, in which the particle (system) is coupled to a set of otherwise free harmonic oscillators (heat bath). Such microscopic system-heat bath models are often referred to as Caldeira-Leggett (CL) models. In many cases they have been exactly solved [4]. The overdamped limit has been derived in these models for the case where the coupling is linear with respect to the oscillator variables but arbitrary with respect to the particle variable [3,5].

A Caldeira-Leggett type model has also been formulated for the case where the system is a self interacting scalar quantum field coupled linearly to a set of otherwise free fields and the overdamped limit has been obtained [6]. This model does provide a microscopic quantum mechanical realization of time-dependent Ginzburg-Landau dynamics in scalar quantum field theory. However, since the couplings between system and environment variables are linear, it should be considered as a first step toward more realistic treatments. More importantly, the calculational method used in [6] cannot be extended to the case when the system variable couples quadratically to other fields.

Although the analysis of overdamping in this paper has general applicability, it was motivated by the warm inflation scenario of the early universe [6,7]. In [7] it was realized that the standard Higgs symmetry breaking scenario, when put into a cosmological setting, provides suitable conditions for the universe to enter a de Sitter expansion phase and then smoothly exit into a radiation dominated phase. The overdamped motion of the order parameter in this scenario may sustain the vacuum energy sufficiently long for de Sitter expansion to solve the horizon and flatness problems. Simultaneously, the relaxational kinetics of the order parameter can maintain the temperature of the universe and permit a smooth exit from the de Sitter phase into the radiation dominated phase. Finally, the thermal fluctuations of the order parameter provide the initial seeds of density perturbations, which in addition could be scale free under specified conditions [7,8]. An elementary analysis of this scenario, based on Friedmann cosmology for general realizations of order parameter kinematics, indicated that if the universe's temperature does not fall too much during de

Sitter expansion, then the cosmological expansion factor from the de Sitter phase should be of order the lower bound set by observation [9]. Although this is not a tight constraint of this scenario, it is a natural one. An analysis of COBE data motivated by this expectation did indicate a slight preference for a small super-Hubble suppression scale, which could be interpreted as arising from a de Sitter expansion with duration near its lower bound [10]. Furthermore, the overdamped limit required by warm inflation, when expressed in different terms, was noted [6] to be an adiabatic limit, for which known methods from dissipative quantum field theory [2,11,14] are presumed valid. These facts provide further motivation to seek a microscopic model of the scenario, which is the goal of the present work.

The calculational methods used here, based on Schwinger's close-time path formalism, were developed in [2]. There are several other works in the literature that apply this formalism to a variety of different situations. [See, for example, the works of Refs. [12–16].] The new feature of the present paper is to shift focus to a kinematic regime dominated by strong dissipation, in order to establish under which conditions this regime leads to overdamped motion. This approach will allow us to have a unique understanding of the microphysical origin of such dynamical behavior, which is in general invoked phenomenologically in applications ranging from condensed matter physics to inflationary cosmology.

The paper is organized as follows. In Sec. II our model of interacting bosons is presented and the effective action is computed perturbatively for a homogeneous time dependent background field configuration  $\phi(t)$ . In Sec. III the effective Langevin-like equation of motion is obtained for  $\phi$  in the symmetry-restored phase. In Sec. IV the overdamped limit of this equation of motion is derived and regions of validity are given. In Sec. V the results of the previous sections, which are for Minkowski space, are extrapolated into a cosmological setting and a preliminary examination is made of the warm inflation scenario. In Sec. VI concluding remarks are given. Two Appendixes are included to clarify a few technical details, like the evaluation of the imaginary part of the self-energies and to stress the importance of taking fully-dressed field propagators to properly describe dissipation in the adiabatic approximation for the field configuration.

## II. MODEL OF INTERACTING BOSONIC FIELDS

### A. The Effective Action

Let us consider the following model of a scalar field  $\phi$  in interaction with  $N$  scalar fields  $\chi_j$ :

$$\mathcal{L}[\phi, \chi_j] = \frac{1}{2}(\partial_\mu \phi)^2 - V[\phi] + \sum_{j=1}^N \left\{ \frac{1}{2}(\partial_\mu \chi_j)^2 - V[\chi_j] \right\} - V_{\text{int}}[\phi, \chi_j], \quad (2.1)$$

where

$$V[\phi] = \frac{m^2}{2}\phi^2 + \frac{\lambda}{4!}\phi^4, \quad (2.2)$$

$$V[\chi_j] = \frac{\mu_j^2}{2}\chi_j^2 + \frac{f_j}{4!}\chi_j^4, \quad (2.3)$$

and

$$V_{\text{int}}[\phi, \chi_j] = \sum_{j=1}^N \frac{g_j^2}{2}\phi^2\chi_j^2. \quad (2.4)$$

For the most part, we will consider all coupling constants positive:  $\lambda, f_j$  and  $g_j^2 > 0$ . Writing  $\phi \rightarrow \varphi + \eta$  in (2.1), where  $\varphi$  is a background field configuration and  $\eta$  are small fluctuations around  $\varphi$ , we obtain the expression for the 1-loop effective action  $\Gamma[\varphi]$ , valid to second order in the fluctuations, by performing the functional (Gaussian) integrations in  $\eta$  and  $\chi_j$ :

$$\Gamma[\varphi] = S[\varphi] + \frac{1}{2}i\text{Tr} \ln [\square + V''(\varphi)] + \frac{1}{2}i \sum_{j=1}^N \text{Tr} \ln [\square + \mu_j^2 + g_j^2\varphi^2], \quad (2.5)$$

where  $S[\varphi] = \int d^4x \mathcal{L}[\varphi, 0]$ ,  $V''(\varphi) = \frac{d^2}{d\phi^2}V[\phi]\Big|_{\phi=\varphi}$ , and

$$\begin{aligned} & \frac{1}{2}i\text{Tr} \ln [\square + V''(\varphi)] + \frac{1}{2}i \sum_{j=1}^N \text{Tr} \ln [\square + \mu_j^2 + g_j^2\varphi^2] = \\ & = -i \ln \int D\eta \prod_j D\chi_j \exp \left\{ -\frac{i}{2}\eta [\square + V''(\varphi)] \eta - \frac{i}{2}\chi_j [\square + \mu_j^2 + g_j^2\varphi^2] \chi_j \right\}. \end{aligned} \quad (2.6)$$

Neglecting contributions to (2.5) which are independent of  $\varphi$ , we can expand the logarithms in (2.5) in powers of  $\varphi$ , obtaining, in the graphic representation:

$$\Gamma[\varphi]_{1\text{-loop}} = \text{diagram 1} + \text{diagram 2} + \sum_{j=1}^N \left[ \text{diagram 3} + \text{diagram 4} \right] + \mathcal{O}(\lambda^3) + \mathcal{O}(g_j^6), \quad (2.7)$$

where we have identified the propagators in the internal lines. External lines are  $\lambda\varphi^2/2$  for the  $\phi$ -graphs and  $g_j^2\varphi^2$  for the  $\chi$ -graphs.

## B. Single-Particle Excitations and Dissipation: Dressing the Propagators

Before presenting our derivation of the effective nonequilibrium equation of motion for  $\varphi$ , we contrast our approach with earlier works in the literature. We closely follow the method of Ref. [2] in the derivation of the evolution equation for  $\varphi$ . In particular, it was shown in [2] that for slowly changing fields, dissipative terms vanish if they are computed perturbatively with bare propagators. There are several issues related to this result. Boyanovsky *et al.* in Ref. [13] argue, in the context of a toy model, that dissipative effects cannot be studied within perturbation theory: perturbation theory breaks down before dissipative effects can be observed. This shows that dissipation is a nonperturbative effect in quantum field theory. In [2] it was shown that dissipative terms can be derived once a consistent “dressing” of propagators is used. This is an explicit way of considering the effect of quasi-particles (or single-particle states) in the evolution of the system, described by  $\varphi$ , in interaction with a thermal bath which represents fluctuations of  $\phi$  and of others fields to which it may be coupled.

It seems reasonable to expect that dissipation effects are closely related to the effect of collisions which dress the field propagators. Take for example the case of a bare propagator expressed in terms of the spectral density  $\rho_0(p)$ , where there is a one to one correspondence between the energy and the momentum of a given state. This completely neglects the spreading of possible energy states due to interactions. In a full “dressing” of propagators, this is accounted for through the introduction of a lifetime (decay width) for single-particle states, such that the full (dressed) spectral density  $\rho(p)$  is smeared out. In particular, particle

lifetimes are crucial in the study of relaxation time-scales in quantum many-body theory [17,18].

Also, the reason why we can get dissipation within our approach can be traced back to the very way that transport coefficients are derived in quantum field theory. As we will show later, the assumption of a slowly moving field is consistent with overdamping in a strong dissipative environment, justifying the adiabatic approximation we adopted. In this regime, there is a close relation between the dissipation we compute and the shear viscosity computed from the Kubo formula [19–22]. As explained in [20,21], diagrams contributing to the shear viscosity have near on-shell singularities for free bare propagators. Full resummed propagators regulate these singularities through an explicit thermal lifetime of single particle excitations. Analogous singularities are exhibited by our expressions for dissipation terms if bare propagators are used. Additional issues concerning the relation of our dissipation terms with the shear viscosity will be discussed in the following two sections.

### C. Self-Energies and Dressed Propagators

From the above discussion, we rewrite the Lagrangian density in (2.1) as

$$\begin{aligned} \mathcal{L} = & \frac{1}{2} (\partial_\mu \phi)^2 - \frac{1}{2} (m^2 + \Sigma_\phi) \phi^2 - \frac{\lambda}{4!} \phi^4 + \frac{1}{2} \Sigma_\phi \phi^2 + \\ & + \sum_{j=1}^N \left\{ \frac{1}{2} (\partial_\mu \chi_j)^2 - \frac{1}{2} (\mu_j^2 + \Sigma_{\chi_j}) \chi_j^2 - \frac{g_j^2}{2} \phi^2 \chi_j^2 - \frac{f_j}{4!} \chi_j^4 + \frac{1}{2} \Sigma_{\chi_j} \chi_j^2 \right\} , \end{aligned} \quad (2.8)$$

where  $\Sigma_\phi$  and  $\Sigma_{\chi_j}$  are the self-energies for the  $\phi$  and  $\chi_j$  fields, respectively. This way we can work with full (dressed) propagators for the  $\phi$  and  $\chi_j$  fields (note the implicit resummation of diagrams involved in this operation) and at the same time keep consistency by considering  $\frac{\lambda}{4!} \phi^4 - \frac{1}{2} \Sigma_\phi \phi^2$  and also  $\frac{f_j}{4!} \chi_j^4 - \frac{1}{2} \Sigma_{\chi_j} \chi_j^2$  as interaction terms. This method has already been adopted before in many different contexts [see, for example [2,22,23]]. In terms of the self-energies the field propagators are written as

$$\frac{1}{q^2 - m^2 + i\epsilon} \longrightarrow \frac{1}{q^2 - m^2 - \Sigma(q) + i\epsilon} . \quad (2.9)$$



For both  $\phi$  and  $\chi_j$  fields, a finite lifetime of single particle excitations, given in terms of the imaginary part of the self-energies, first appear at the two-loop order. We thus restrict, for simplicity, the evaluation of  $\Sigma_\phi$  and  $\Sigma_{\chi_j}$  up to the two-loop level. Diagrammatically, the self-energies are given by

$$\begin{aligned} \Sigma_\phi = & \text{[diagram: circle with } \phi \text{ on top]} + \text{[diagram: circle with } \chi \text{ on top]} + \text{[diagram: two circles, top } \phi \text{, bottom } \phi \text{, left } \phi \text{, right } \phi]} + \text{[diagram: two circles, top } \phi \text{, bottom } \chi \text{, left } \chi \text{, right } \chi]} \\ & + \text{[diagram: two circles, top } \chi \text{, bottom } \chi \text{, left } \chi \text{, right } \chi]} + \text{[diagram: two circles, top } \chi \text{, bottom } \phi \text{, left } \phi \text{, right } \phi]} + \text{[diagram: two circles, top } \phi \text{, bottom } \phi \text{, left } \phi \text{, right } \phi]} \\ & + \text{[diagram: circle with } \phi \text{ on top and bottom, horizontal line through center]} + \text{[diagram: circle with } \chi \text{ on top and bottom, horizontal line through center]} + \text{higher loop terms} \end{aligned} \quad (2.10)$$

and

$$\begin{aligned} \Sigma_\chi = & \text{[diagram: circle with } \chi \text{ on top]} + \text{[diagram: circle with } \phi \text{ on top]} + \text{[diagram: two circles, top } \chi \text{, bottom } \chi \text{, left } \chi \text{, right } \chi]} + \text{[diagram: two circles, top } \phi \text{, bottom } \chi \text{, left } \chi \text{, right } \chi]} \\ & + \text{[diagram: two circles, top } \phi \text{, bottom } \phi \text{, left } \phi \text{, right } \phi]} + \text{[diagram: two circles, top } \chi \text{, bottom } \phi \text{, left } \phi \text{, right } \phi]} + \text{[diagram: circle with } \chi \text{ on top and bottom, horizontal line through center]} \\ & + \text{[diagram: circle with } \phi \text{ on top and bottom, horizontal line through center]} + \text{higher loop terms.} \end{aligned} \quad (2.11)$$

The setting sun (non-local) diagrams in (2.10) and (2.11) (the two last terms in (2.10) and (2.11)) contribute imaginary terms to the self-energies, from which we can write the decay widths  $\Gamma_\phi$ ,  $\Gamma_{\chi_j}$ , for the  $\phi$  and  $\chi_j$  fields, respectively, in terms of the on-shell expressions [21–23] ( $\Sigma_I \equiv \text{Im}\Sigma$ ):

$$\Gamma_\phi(q) = \frac{\Sigma_I^\phi(\mathbf{q}, \omega_\phi)}{2\omega_\phi} \quad (2.12)$$

and

$$\Gamma_{\chi_j}(q) = \frac{\Sigma_I^{\chi_j}(\mathbf{q}, \omega_{\chi_j})}{2\omega_{\chi_j}}, \quad (2.13)$$

where  $\omega_{\phi(\chi_j)}$  is given by the solution of  $\omega^2 = \mathbf{q}^2 + m^2 + \text{Re}\Sigma(\mathbf{q}, \omega)$ .

Explicit expressions for  $\Gamma(q)$  in the  $\lambda\phi^4$  model have been obtained in [21] and [22]. We follow [21] to compute  $\Gamma_\phi$  and  $\Gamma_{\chi_j}$ . A straightforward extension of the computation can be

applied to our model of interacting  $\phi$ – $\chi_j$  fields. Some of the details are shown in Appendix A, where we evaluate the imaginary contribution coming from the mixed setting sun diagrams in  $\Sigma_\phi$  and  $\Sigma_{\chi_j}$  [the last diagrams in (2.10) and (2.11)]. Even though in general there are no simple way of expressing the results, if we adopt the zero space momentum ( $|\mathbf{q}| = 0$ ) approximation for the imaginary part of the self-energies, we can find simple approximated expressions for both (2.12) and (2.13), respectively, given at finite temperature ( $\beta = 1/T$ ) by (for  $m_T \sim \mathcal{O}(\mu_j(T))$ )

$$\begin{aligned} \Gamma_\phi(q)|_{\Sigma_I^\phi(0,m_T)} &\sim \frac{\lambda^2 T^2}{2^8 \pi^3 \omega_\phi(\mathbf{q})} \text{Li}_2(1 - e^{-\beta m_T}) \\ &+ \left(1 + \frac{1}{2} \delta_{\phi,\chi_j}\right) \sum_{j=1}^N \frac{g_j^4 T^2}{2^5 \pi^3 \omega_\phi(\mathbf{q})} \left[ \text{Li}_2(1 - e^{-\beta m_T}) - \text{Li}_2\left(\frac{1 - e^{-\beta m_T}}{1 - e^{-\beta \mu_j(T)}}\right) \right] \end{aligned} \quad (2.14)$$

and

$$\begin{aligned} \Gamma_{\chi_j}(q)|_{\Sigma_I^{\chi_j}(0,\mu_j(T))} &\sim \frac{f_j^2 T^2}{2^8 \pi^3 \omega_{\chi_j}(\mathbf{q})} \text{Li}_2(1 - e^{-\beta \mu_j(T)}) \\ &+ \left(1 + \frac{1}{2} \delta_{\phi,\chi_j}\right) \frac{g_j^4 T^2}{2^5 \pi^3 \omega_{\chi_j}(\mathbf{q})} \left[ \text{Li}_2(1 - e^{-\beta \mu_j(T)}) - \text{Li}_2\left(\frac{1 - e^{-\beta \mu_j(T)}}{1 - e^{-\beta m_T}}\right) \right] . \end{aligned} \quad (2.15)$$

In the above expressions,  $m_T$  and  $\mu_j(T)$  are the thermal masses for  $\phi$  and  $\chi_j$ , respectively.  $\delta_{\phi,\chi_j} = 1$  for  $m_T = \mu_j(T)$  and  $\delta_{\phi,\chi_j} = 0$  otherwise.  $\text{Li}_2(z)$  is the dilogarithm function<sup>1</sup>.

This approximation for the decay widths, in terms of the zero space-momentum expression for the imaginary part of the self-energies, is common to computations of transport coefficients and contrast densities in field theory [11,19,20]. However, Wang, Heinz and Zhang [22] showed that this approximation may lead to errors in the calculation of the contrast density in the  $\lambda\phi^4$  model. In fact, the expressions for  $\text{Im}\Sigma$  can be fast changing for some momentum range and values of the masses. For example, in Fig. 1 we plot the value of (the on-shell)  $\text{Im}\Sigma(q)$ , obtained numerically, as a function of the momentum, normalized by

---

<sup>1</sup>We follow the convention in Ref. [24] for the definition of the dilogarithm function:  $\text{Li}_2(z) = -\int_1^z \frac{\ln t}{t-1} dt$ . Some useful approximations for  $\text{Li}_2(z)$  are  $\text{Li}_2(z) \sim \frac{\pi^2}{6} + [\ln(z) - 1]z + \mathcal{O}(z^2)$ , for  $z \ll 1$ , and  $\text{Li}_2(z) \sim -\frac{\pi^2}{6} - \frac{1}{2} \ln^2(z) + \mathcal{O}(1/z)$ , for  $z \gg 1$ .

its  $|\mathbf{q}| = 0$  expression (for  $f_j \ll g_j^2$ ). Even though  $\text{Im}\Sigma(q)$  can depart considerable from its  $|\mathbf{q}| = 0$  value, we will show later that, for a range of small thermal masses, this approximation results in a small error ( $\lesssim 10\%$ ) in the expression for the dissipation coefficient, when compared with the computation using the complete  $|\mathbf{q}| \neq 0$  expressions for  $\text{Im}\Sigma(q)$ .

In the analysis presented in the next sections, it will also be sufficient to use the leading order high temperature expressions for the finite temperature effective (renormalized) masses,  $m_T$  and  $\mu_j(T)$ , appearing in (2.12) - (2.15), (obtained from the 1-loop diagrams in (2.10) and (2.11), respectively), given by<sup>2</sup>

$$m_T^2 = m^2 + \text{Re}\Sigma_\phi(m_T) \stackrel{T \gg m}{\sim} m^2 + \frac{\lambda T^2}{24} + \sum_{j=1}^N g_j^2 \frac{T^2}{12} \quad (2.16)$$

and

$$\mu_j^2(T) = \mu_j^2 + \text{Re}\Sigma_{\chi_j}(\mu_j(T)) \stackrel{T \gg \mu_j}{\sim} \mu_j^2 + \frac{f_j T^2}{24} + g_j^2 \frac{T^2}{12}. \quad (2.17)$$

#### D. Real-Time Full Field Propagators

In order to obtain the evolution equation for the field configuration  $\varphi$ , we use the real-time Schwinger's closed-time path (CTP) formalism [25]. In the CTP formalism the time integration is along a contour  $c$  from  $-\infty$  to  $+\infty$  and then back to  $-\infty$ . For reviews please see, for example, refs. [26–28].

In the CTP formalism the field propagators are given by [2] (with analogous expressions for  $G_{\chi_j}$ ):

---

<sup>2</sup>The divergences in (2.10) and (2.11), as in the effective action, can be dealt with by the usual introduction of the appropriate renormalization counterterms in the initial Lagrangian, for the masses, coupling constants and the wave-function. In particular, we note that the imaginary terms in the self-energies expressions, coming from the setting-sun diagrams, are finite.  $m$ ,  $\mu$ ,  $g$ ,  $f$  and  $\lambda$  in (2.16) and (2.17) and in our later results are to be interpreted as the corrected and not as bare quantities.

$$\begin{aligned}
G_\phi^{++}(x, x') &= i\langle T_+ \phi(x) \phi(x') \rangle \\
G_\phi^{--}(x, x') &= i\langle T_- \phi(x) \phi(x') \rangle \\
G_\phi^{+-}(x, x') &= i\langle \phi(x') \phi(x) \rangle \\
G_\phi^{-+}(x, x') &= i\langle \phi(x) \phi(x') \rangle,
\end{aligned} \tag{2.18}$$

where  $T_+$  and  $T_-$  indicate chronological and anti-chronological ordering, respectively.  $G_\phi^{++}$  is the usual physical (causal) propagator. The other three propagators come as a consequence of the time contour and are considered as auxiliary (unphysical) propagators. The expressions for  $G_\phi^{n,l}(x, x')$  in terms of its momentum-space Fourier transforms are given by

$$G_\phi(x, x') = i \int \frac{d^3 q}{(2\pi)^3} e^{i\mathbf{q} \cdot (\mathbf{x} - \mathbf{x}')} \begin{pmatrix} G_\phi^{++}(\mathbf{q}, t - t') & G_\phi^{+-}(\mathbf{q}, t - t') \\ G_\phi^{-+}(\mathbf{q}, t - t') & G_\phi^{--}(\mathbf{q}, t - t') \end{pmatrix}, \tag{2.19}$$

where

$$\begin{aligned}
G_\phi^{++}(\mathbf{q}, t - t') &= G_\phi^>(\mathbf{q}, t - t')\theta(t - t') + G_\phi^<(\mathbf{q}, t - t')\theta(t' - t) \\
G_\phi^{--}(\mathbf{q}, t - t') &= G_\phi^>(\mathbf{q}, t - t')\theta(t' - t) + G_\phi^<(\mathbf{q}, t - t')\theta(t - t') \\
G_\phi^{+-}(\mathbf{q}, t - t') &= G_\phi^<(\mathbf{q}, t - t') \\
G_\phi^{-+}(\mathbf{q}, t - t') &= G_\phi^>(\mathbf{q}, t - t')
\end{aligned} \tag{2.20}$$

In terms of the decay width  $\Gamma_\phi$ , the expression for the full dressed propagators at finite temperature where obtained in [2], from which we have

$$\begin{aligned}
G_\phi^>(\mathbf{q}, t - t') &= \frac{1}{2\omega_\phi} \left\{ [1 + n(\omega_\phi - i\Gamma_\phi)] e^{-i(\omega_\phi - i\Gamma_\phi)(t - t')} + n(\omega_\phi + i\Gamma_\phi) e^{i(\omega_\phi + i\Gamma_\phi)(t - t')} \right\} \\
G_\phi^<(\mathbf{q}, t - t') &= G_\phi^>(\mathbf{q}, t' - t),
\end{aligned} \tag{2.21}$$

where  $n(\omega) = (e^{\beta\omega} - 1)^{-1}$  is the Bose distribution and  $\omega \equiv \omega(\mathbf{q})$  is the particle's energy, or dispersion relation,  $\omega_\phi(\mathbf{q}) = \sqrt{\mathbf{q}^2 + m_T^2}$ . For  $G_{\chi_j}$ ,  $\omega_{\chi_j}(\mathbf{q}) = \sqrt{\mathbf{q}^2 + \mu_j^2(T)}$ .

### III. DISSIPATION IN THE ADIABATIC REGIME

### A. The Effective Equation of Motion

With fields in the forward and backward segments of the CTP time contour identified as  $\phi_+, \chi_+$  and  $\phi_-, \chi_-$ , respectively, the classical action can be written as

$$S[\phi, \chi] = \int d^4x \{ \mathcal{L}[\phi_+, \chi_+] - \mathcal{L}[\phi_-, \chi_-] \} , \quad (3.1)$$

The evaluation of the effective action at real time can be done exactly as in [2]. There are also a number of other works using Schwinger's closed-time path formalism to obtain the real-time effective action for field configurations. [See. e.g., Refs. [13–16].] Here we will concentrate on the evaluation of the effective equation of motion in the strong dissipative regime. In the evaluation of the effective action there appear several imaginary terms, once the  $\chi$  fields and the fluctuations around the  $\varphi$  background are integrated out. These imaginary terms can be interpreted as coming from functional integrations over Gaussian stochastic fields, as can be visualized by introducing the new field variables:

$$\varphi_c = \frac{1}{2} (\phi_+ + \phi_-) , \quad \varphi_\Delta = \phi_+ - \phi_- . \quad (3.2)$$

In terms of these new variables the equation of motion is obtained by [2,14]

$$\frac{\delta S_{\text{eff}}[\varphi_\Delta, \varphi_c, \xi_j]}{\delta \varphi_\Delta} \Big|_{\varphi_\Delta=0} = 0 , \quad (3.3)$$

where  $\xi_j$  are stochastic fields, related to each distinct dissipative kernel appearing in (3.3).

At 1-loop order, the leading contributions to the dissipative terms in the equation of motion come from the diagrams:

$$\begin{array}{c} \phi \\ \diagup \quad \diagdown \\ \text{---} \bigcirc \text{---} \\ \diagdown \quad \diagup \\ \phi \end{array} + \sum_{j=1}^N \left[ \begin{array}{c} \chi_j \\ \diagup \quad \diagdown \\ \text{---} \bigcirc \text{---} \\ \diagdown \quad \diagup \\ \chi_j \end{array} \right] \quad (3.4)$$

The explicit expression corresponding to these terms appearing in the effective equation of motion, Eq. (3.3), is (as obtained in [2] for a similar case)

$$\begin{aligned}
& \varphi_c(x) \int d^4x' \varphi_c^2(x') \left\{ \frac{\lambda^2}{2} \text{Im} [G_\phi^{++}]_{x,x'}^2 + \sum_{j=1}^N 2g_j^4 \text{Im} [G_{\chi_j}^{++}]_{x,x'}^2 \right\} \theta(t-t') \\
& \sim \varphi_c^2(t) \dot{\varphi}_c(t) \left\{ \frac{\lambda^2}{8} \beta \int \frac{d^3q}{(2\pi)^3} \frac{n_\phi(1+n_\phi)}{\omega_\phi^2(\mathbf{q}) \Gamma_\phi(\mathbf{q})} + \sum_{j=1}^N \frac{g_j^4}{2} \beta \int \frac{d^3q}{(2\pi)^3} \frac{n_{\chi_j}(1+n_{\chi_j})}{\omega_{\chi_j}^2(\mathbf{q}) \Gamma_{\chi_j}(\mathbf{q})} \right\} \\
& + \mathcal{O} \left( \lambda^2 \frac{\Gamma_\phi}{\omega_\phi} \right) + \mathcal{O} \left( g_j^4 \frac{\Gamma_{\chi_j}}{\omega_{\chi_j}} \right) \\
& + \varphi_c^3(t) \int_{-\infty}^t dt' \int \frac{d^3q}{(2\pi)^3} \left\{ \frac{\lambda^2}{2} \text{Im} [G_\phi^{++}(\mathbf{q}, t-t')]^2 + 2 \sum_{j=1}^N g_j^4 \text{Im} [G_{\chi_j}^{++}(\mathbf{q}, t-t')]^2 \right\}, \quad (3.5)
\end{aligned}$$

where in the lhs of the above equation, we used the compact notation

$$[G_{\phi, \chi_j}^{++}]_{x,x'}^2 = \int \frac{d^3k}{(2\pi)^3} \exp[i\mathbf{k} \cdot (\mathbf{x} - \mathbf{x}')] \int \frac{d^3q}{(2\pi)^3} G_{\phi, \chi_j}^{++}(\mathbf{q}, t-t') G_{\phi, \chi_j}^{++}(\mathbf{q} - \mathbf{k}, t-t'), \quad (3.6)$$

with  $G^{++}(\mathbf{q}, t-t')$  obtained from (2.20) and (2.21). In the rhs of (3.5), we have taken the limit of homogeneous fields, for details see the Appendix B. We have also made use of the approximation for slowly moving fields:  $\varphi_c^2(t') - \varphi_c^2(t) \sim 2\varphi_c(t)\dot{\varphi}_c(t)(t' - t)$ . In the next section we show that this approximation is consistent with strong dissipation. After performing the time integration and retaining the leading terms in the coupling constants, we obtain the result given in (3.5). The last term, proportional to  $\varphi_c^3$ , will correspond to the finite temperature correction to the quartic  $\phi$  self-interaction (see Appendix B).

The final equation of motion, at leading order in the coupling constants, at high temperatures ( $\mu_j(T), m_T \ll T$ ) and in the adiabatic limit, can then be written as

$$\ddot{\varphi}_c + m_T^2 \varphi_c(t) + \frac{\lambda_T}{3!} \varphi_c^3(t) + \eta_1 \varphi_c^2(t) \dot{\varphi}_c(t) = \varphi_c(t) \xi_1(t), \quad (3.7)$$

where  $m_T$  is given by (2.16),  $\lambda_T$  is the temperature-dependent effective (renormalized) quartic coupling constant<sup>3</sup>:

---

<sup>3</sup>The terms linear in the temperature come from the two-vertex diagrams in (3.4). The apparent instability from these terms for high  $T$  is only an artifact of the loop expansion. As shown in [29] for the  $\phi^4$  model, once higher order corrections are accounted for,  $\lambda_T$  is always positive even in the  $T \rightarrow \infty$  limit. Using full dressed propagators we are automatically taking into account these higher

$$\begin{aligned}
\lambda_T \simeq & \lambda - \frac{3\lambda^2}{2} \left\{ \frac{T}{8\pi m_T} + \frac{1}{8\pi^2} \left[ \ln \left( \frac{m_T}{4\pi T} \right) + \gamma \right] + \mathcal{O} \left( \frac{m}{T} \right) \right\} - \\
& - 6 \sum_{j=1}^N g_j^4 \left\{ \frac{T}{8\pi \mu_j(T)} + \frac{1}{8\pi^2} \left[ \ln \left( \frac{\mu_j(T)}{4\pi T} \right) + \gamma \right] + \mathcal{O} \left( \frac{\mu_j(T)}{T} \right) \right\} + \\
& + \mathcal{O}(\lambda^3, g^4 f, \lambda^2 g^2, g^6),
\end{aligned} \tag{3.8}$$

In (3.7),  $\xi_1$  is a stochastic field associated with the imaginary terms in the effective action coming from the real-time evaluation of the diagrams (3.4). Its two-point correlation function is given by [2]

$$\langle \xi_1(x) \xi_1(x') \rangle = \frac{\lambda^2}{2} \text{Re} \left[ G_{\phi}^{++} \right]_{x,x'}^2 + 2 \sum_{j=1}^N g_j^4 \text{Re} \left[ G_{\chi_j}^{++} \right]_{x,x'}^2. \tag{3.9}$$

Note that since we are considering homogeneous field configurations,  $\xi_1$  is a space uncorrelated stochastic field, but it is colored (time dependent) and Gaussian distributed, with probability distribution given by ( $N_1$  is a normalization constant)

$$P[\xi_1] = N_1^{-1} \exp \left\{ -\frac{1}{2} \int d^4x d^4x' \xi_1(x) \left[ \frac{\lambda^2}{2} \text{Re} \left[ G_{\phi}^{++} \right]_{x,x'}^2 + 2 \sum_j g_j^4 \text{Re} \left[ G_{\chi_j}^{++} \right]_{x,x'}^2 \right]^{-1} \xi_1(x') \right\}. \tag{3.10}$$

As shown in [2], the dissipative coefficient in (3.7), written explicitly in Eq. (3.12) below, and the noise correlation function Eq. (3.9) (in the homogeneous limit), are related by a fluctuation-dissipation expression valid within our approximations (1-loop order at  $\lambda^2, g_j^4$  and for  $\Gamma/\omega \ll 1$ ,  $\Gamma/T \ll 1$ ):

$$\eta_1 = \frac{1}{2T} \int d^4x' \langle \xi_1(x) \xi_1(x') \rangle. \tag{3.11}$$

In [2] it was also shown that as  $T \rightarrow \infty$ ,  $\Gamma_{\phi, \chi_j} \rightarrow \infty$ , and the integrand in (3.9) becomes sharply peaked at  $|t - t'| \sim 0$ . In this limit, we can obtain an approximate Markovian limit for (3.9).

---

order corrections, through the appearance of thermal masses in (3.8). However, in the multi-field case there is the possibility of vacuum instability due to the  $\phi$  couplings to the  $\chi_j$  fields. This appears as a constraint in our estimates below.

We can read the dissipation coefficient  $\eta_1$ , which appears in Eq. (3.7), from (3.5)<sup>4</sup>,

$$\eta_1 = \frac{\lambda^2}{8}\beta \int \frac{d^3q}{(2\pi)^3} \frac{n_\phi(1+n_\phi)}{\omega_\phi^2(\mathbf{q})\Gamma_\phi(\mathbf{q})} + \sum_{j=1}^N \frac{g_j^4}{2}\beta \int \frac{d^3q}{(2\pi)^3} \frac{n_{\chi_j}(1+n_{\chi_j})}{\omega_{\chi_j}^2(\mathbf{q})\Gamma_{\chi_j}(\mathbf{q})} + \mathcal{O}\left(\lambda^2 \frac{\Gamma_\phi}{\omega_\phi}, g_j^4 \frac{\Gamma_{\chi_j}}{\omega_{\chi_j}}\right). \quad (3.12)$$

For the model we are interested in, with Lagrangian density given by (2.1), with a large number of  $\chi$  fields coupled to  $\phi$ , and for  $f_j \ll g_j^2$  and  $\lambda \lesssim g_j$ , we can use the obtained expressions for  $\Gamma_\phi$  and  $\Gamma_{\chi_j}$ , to show that  $\Gamma_\phi \gg \Gamma_{\chi_j}$ . Since the dissipation coefficient, Eq. (3.12), goes as  $1/\Gamma$ ,  $\Gamma_{\chi_j}$  will give the dominant contribution to  $\eta_1$ . An explicit expression for  $\eta_1$ , can be obtained by using the  $|\mathbf{q}| = 0$  approximation for  $\text{Im}\Sigma_\phi(q)$  and  $\text{Im}\Sigma_{\chi_j}(q)$ , or, equivalently, Eqs. (2.14) and (2.15) for  $\Gamma_\phi$  and  $\Gamma_{\chi_j}$ , respectively, in Eq. (3.12). At the high temperature limit,  $T \gg m_T, \mu_j(T)$  and for  $m_T \sim \mathcal{O}(\mu_j(T))$ , we then obtain the following approximate expression for  $\eta_1$  (using  $\text{Li}_2(z) \sim \pi^2/6$ , for  $z \ll 1$ )

$$\eta_1 \stackrel{T \gg m_T, \mu_j(T)}{\simeq} \frac{96}{\pi T} \left\{ \frac{\lambda^2}{8\lambda^2 + \sum_{j=1}^N g_j^4 \left[1 - \frac{6}{\pi^2} \text{Li}_2\left(\frac{m_T}{\mu_j(T)}\right)\right]} \ln\left(\frac{2T}{m_T}\right) + \sum_{j=1}^N \frac{4g_j^4}{f_j^2 + 8g_j^4 \left[1 - \frac{6}{\pi^2} \text{Li}_2\left(\frac{\mu_j(T)}{m_T}\right)\right]} \ln\left(\frac{2T}{\mu_j(T)}\right) \right\}. \quad (3.13)$$

In order to test the validity of the above approximate expression for  $\eta_1$ , we have computed it numerically. The two expressions are shown in Fig. 2, for  $f_j \ll g_j^2$ ,  $\lambda \lesssim g_j$ , and  $N = 25$ , where, for simplicity, we have also considered  $\mu_j = \mu$  and  $g_j = g$  for all  $\chi_j$  fields ( $m_T \sim 5\mu_j(T)$ ). We see that the above approximation for  $\eta_1$  fits reasonably well the full expression for the dissipation coefficient in the high temperature region, having a  $\lesssim 10\%$  discrepancy for  $m_T/T \lesssim 0.4$ .

---

<sup>4</sup>In [2] an extra contribution to the  $\phi$  decay rate coming from the  $\phi - \chi$  interaction was left out. Here we give the correct expressions for  $\Gamma_\phi$ ,  $\Gamma_\chi$  and for the dissipation.



## B. Dissipation Coefficient and Shear Viscosity

It is interesting to note the close relation of the above expression for the dissipation coefficient with that obtained for the shear viscosity evaluated, *e.g.*, from a Kubo formula [19–21]:

$$\eta_{\text{shear}} = i \int d^3\mathbf{x} \int_{-\infty}^0 dt \int_{-\infty}^t dt' \langle [\pi_{kl}(0), \pi_{kl}(\mathbf{x}, t')] \rangle , \quad (3.14)$$

where  $\pi_{kl} = (\delta_i^k \delta_l^j - \frac{1}{3} \delta_l^k \delta_i^j) T_j^i$ , with  $T_j^i$  the space components of the energy-momentum tensor. In our case, with Lagrangian given by (2.1),

$$T_\nu^\mu = \frac{\partial \mathcal{L}}{\partial(\partial_\mu \phi)} \partial_\nu \phi + \sum_j \frac{\partial \mathcal{L}}{\partial(\partial_\mu \chi_j)} \partial_\nu \chi_j - \delta_\nu^\mu \mathcal{L} . \quad (3.15)$$

In order to compute the shear viscosity in (3.14) to lowest order, we must evaluate the diagrams (3.4), which, as shown in [20,21], have near on-shell singularities coming from the product of (bare) propagators. These singularities are softened once explicit lifetimes for excitations are included through dressed propagators. Taking this into account, we obtain the following expression for the shear viscosity  $\eta_{\text{shear}}$  (in analogy with the evaluation of  $\eta_{\text{shear}}$  in the  $\lambda\phi^4$  single field case),

$$\eta_{\text{shear}} \stackrel{T \gg m_T, \mu_j(T)}{\simeq} \frac{\beta}{30} \int \frac{d^3k}{(2\pi)^3} |\mathbf{k}|^4 \left[ \frac{n_\phi(1+n_\phi)}{\omega_\phi^2 \Gamma_\phi} + \sum_j \frac{n_{\chi_j}(1+n_{\chi_j})}{\omega_{\chi_j}^2 \Gamma_{\chi_j}} \right] . \quad (3.16)$$

Compare the above expression with (3.12). The evaluation of (3.16) leads to the standard result for the shear viscosity being proportional to  $T^3$  and inversely proportional to the coupling constants. However, Eq. (3.16), as shown by Jeon in [21], does not represent the unique contribution to  $\eta_{\text{shear}}$  at this order of coupling constants. Due to the near on-shell singularities and the way they are regulated by the thermal width, there is an entire class of diagrams, called ladder diagrams (diagrams with insertions of loops between the two propagators in (3.4)), contributing to  $\eta_{\text{shear}}$  at the same order. By using a formal resummation of vertices, Jeon was able to perform the summation of the whole set of ladder diagrams in the simple  $\lambda\phi^4$  theory, showing that the true value of the shear viscosity is

about four times larger than the one loop result in the high temperature limit. Since our expression for the dissipation coefficient exhibits the same properties of  $\eta_{\text{shear}}$ , we expect that these higher loop ladder diagrams will also give a significant contribution to the value of  $\eta_1$  in (3.12). However, as we are dealing with the more complicated situation of several interacting fields, we will not attempt here to evaluate these contributions. From the example of the shear viscosity calculation in the single field case, these ladder contributions will only add to the one-loop result for the dissipation coefficient, not changing qualitatively our results. Thus, Eq. (3.12) represents, at least, a *lower bound* for the dissipation, applicable in the strong dissipation regime, as we will show next.

#### IV. ADIABATIC APPROXIMATION AND STRONG DISSIPATION

We now investigate the validity and limits of applicability of our main approximations, in particular the adiabatic approximation. In order to arrive at the expression for the dissipation, Eq. (3.12), and to write the equation of motion for  $\varphi_c$  as in Eq. (3.7), we assumed that the field  $\varphi_c$  changes adiabatically [see (3.5)]:

$$\varphi_c^2(t') - \varphi_c^2(t) \simeq 2(t' - t)\varphi_c(t)\dot{\varphi}_c(t) + \text{higher time derivative terms} . \quad (4.1)$$

This approximation for the field configuration has recently been the focus of some attention in the literature [15]. The authors in [15], working with soft field modes set by a coarse graining scale  $k_c$ , showed that the adiabatic approximation breaks down once the field configurations (soft modes) oscillate with the same time scale as the dissipative kernels (with time scale given by  $\sim k_c^{-1}$ ). However, here we work in a very different context. We are mainly concerned with the overdamped motion of the homogeneous field configuration  $\varphi_c$ , *i.e.*, when its oscillatory motion is suppressed. Therefore, the dynamic time-scale for  $\varphi_c$  must be much larger than the typical collision time-scale ( $\sim \Gamma^{-1}$ ). Note that this is a much stronger condition than the simple requirement that the field should change slowly in time, with time scale set by the frequency  $\omega(\mathbf{k}) = \sqrt{\mathbf{k}^2 + m_T^2}$ . Thus, we must examine when the condition

$$\left| \frac{\varphi_c}{\dot{\varphi}_c} \right| \gg \Gamma^{-1} \quad (4.2)$$

is satisfied.

We choose  $\Gamma$  as the smallest of the two thermal decay widths  $\Gamma_\phi$ ,  $\Gamma_{\chi_j}$ , as it will set the largest time-scale for collisions for the system in interaction with the thermal bath.

Note that in the evaluation of the dissipation coefficient in (3.5), the leading contribution to the first time derivative of  $\varphi_c$  is of order  $\Gamma^{-1}$ . As discussed earlier in connection with the shear viscosity coefficient, the dependence of the dissipation coefficient on the decay width  $\Gamma$  comes from using it as the regulator of on-shell singularities present in (3.4) at first order in the time derivative. In Appendix B we present an argument justifying the need of regulating with the decay width and also compute the next order contribution in the adiabatic approximation, showing the consistency of the results.

Since the stronger the dissipation the more efficient the adiabatic approximation, the parameter range where (4.2) is valid leads naturally to the regime where  $\varphi_c$  undergoes overdamped motion (in the sense of Eq. (4.4) below). If we consider the ensemble average of the equation of motion (3.7):

$$\left\langle \frac{\delta S_{\text{eff}}[\varphi_\Delta, \varphi_c, \xi_j]}{\delta \varphi_\Delta} \Big|_{\varphi_\Delta=0} \right\rangle = 0, \quad (4.3)$$

where  $\langle \dots \rangle$  means average over the stochastic fields, then we define the overdamped regime when the (averaged) background configuration  $\varphi_c$  satisfies

$$\eta_1 \varphi_c^2 \dot{\varphi}_c + m_T^2 \varphi_c + \frac{\lambda_T}{6} \varphi_c^3 = 0. \quad (4.4)$$

We also restrict our study to the high-temperature and ultra-relativistic region:  $T \sim |\mathbf{q}| \gg m_T, \mu_j(T)$ . We take the couplings  $g_j, f_j$  such that  $g_j^2 \gg f_j$ . Also, for simplicity, as before, we take all  $g_j = g$ . At high temperatures we can then write for (2.16) and (2.17) ( $T^2 \gtrsim 24m^2/\lambda, 12\mu^2/g^2$ ) the expressions

$$m_T^2 \sim (\lambda + 2Ng^2) \frac{T^2}{24}, \quad (4.5)$$

where  $N$  is the number of fields coupled to  $\phi$ , and

$$\mu_T^2 \sim g^2 \frac{T^2}{12} . \quad (4.6)$$

### A. Results for three different cases

We will examine the condition for strong dissipation with overdamped motion for three particular choices of parameters, showing that there is a region of parameter space consistent with this regime. Using (4.4), we can write the equivalent expression for (4.2):

$$\left| \frac{m_T^2 + \frac{\lambda_T}{6} \varphi_c^2}{\eta_1 \varphi_c^2} \right| \ll \Gamma_\chi . \quad (4.7)$$

In the estimates below, we evaluated both  $\eta_1$  [from Eq. (3.12)], and  $\Gamma_\chi$  (computed at  $|\mathbf{q}| = T$ ) numerically. The three cases analyzed are:

**Case 1:**  $\lambda \sim g^2$ : In this case we obtain that

$$m_T^2 \sim (1 + 2N) g^2 \frac{T^2}{24} , \quad (4.8)$$

$$\lambda_T \gtrsim g^2 \left( 1 - \frac{3\sqrt{3}Ng}{2\pi} \right) . \quad (4.9)$$

Note that the last condition is written as a constraint for the positivity of  $\lambda_T$ . With these values and for the case  $N = 25$ , we obtain the results shown in Fig. 3a, where we have plotted both sides of Eq. (4.7). The region of parameters satisfying Eq. (4.7) is given by the intersection of the region below the solid lines (the function  $\Gamma_\chi$ ) with the region above the dashed line ( $|\dot{\varphi}_c/\varphi_c|$  computed for different values of  $\varphi_c$ ).

**Case 2:**  $\lambda \sim g$ : As above, this is shown in Fig. 3b. The region satisfying Eq. (4.7) is given again by the intersecting region below the solid line and above the dashed lines.

In both Figs. 3a and 3b, the results are shown up to the value of  $m_T$  satisfying the constraint for the positivity of  $\lambda_T$ .

**Case 3:**  $\lambda_T \approx g^4$ : This case follows a slightly different philosophy, of fixing the corrected coupling as opposed to the bare coupling. We have,

$$\lambda \approx g^4 + \frac{3\sqrt{3}Ng^3}{2\pi} \equiv \lambda(g, N) , \quad (4.10)$$

$$m_T^2 \sim \left( \lambda(g, N) + 2Ng^2 \right) \frac{T^2}{24} , \quad (4.11)$$

with the additional constraint,

$$\lambda(g, N) < 1 . \quad (4.12)$$

The results for this case are shown in Fig. 3c, with the same interpretation as in cases 1 and 2: the region satisfying Eq. (4.7) is given by the intersecting region below the solid line and above the dashed lines. The results are shown up to the value for  $m_T$  satisfying the condition (4.12).

We note that the case  $\lambda_T \approx g^4$  is the one with the broadest range of validity in parameter space, as seen in Fig. 3c, followed by the case  $\lambda \approx g$ , shown in Fig. 3b. For  $\lambda = g^2$ , the condition for adiabaticity is only possible for fairly large field amplitudes, which may be beyond the validity of a perturbative evaluation of the effective action. We will come back to this issue in the next section. In any case, we stress that there are several regimes where the adiabatic approximation is valid.

In all cases, the smaller  $N$  the smaller the region of parameters that satisfies (4.2). In particular, for  $N < 2$ , we find no parameter range satisfying (4.2) and therefore, the adiabatic approximation. This is consistent with the intuition that dissipation is caused by the decay of the  $\phi$  field into  $\chi$  fields and is more efficient the larger the number of decay channels available. We also obtain that  $\varphi_c$  is always somewhat large ( $\gtrsim 2T$ ) for the range of physical parameters satisfying (4.2), for both cases analyzed, being even higher for case 1.

If in (4.7) we use  $\Gamma_\phi$  instead of  $\Gamma_{\chi_j}$ , the region of parameters improves considerably; since  $\Gamma_\phi \gg \Gamma_{\chi_j}$  for large  $N$ , it allows much smaller values of  $\varphi_c/T$ . It should be recalled that  $\Gamma_\phi$  determines the relaxation time scale for the  $\phi$  field.

Finally, as discussed earlier, the expression we quoted for  $\eta_1$  gives only a lower bound for the dissipation coefficient. As in the case studied by Jeon in [21], higher loop ladder

diagrams can lead to a considerably higher value for  $\eta_1$ . For several interacting fields, simple estimates show that these ladder diagrams scale at most as  $N$ . Therefore, they may well be of the same order as the leading order 1-loop contribution to the dissipation coefficient, given by the  $\chi$ -sector. We leave a more detailed analysis of the contributions coming from ladder diagrams to a future work. Additional contributions to the dissipation coefficient in (3.12) only improve our estimates, enlarging the region of parameter space satisfying the adiabatic approximation; the ratio  $\varphi_c/T$  decreases, broadening the conditions under which the field undergoes overdamped motion (strong dissipative regime).

It is worth mentioning that the  $\phi - \chi$  coupling constant in Eq. (2.1) can be negative and this also leads to interesting results. As an illustrative example, consider an even number of  $\chi$ -fields with the sign of the  $\phi - \chi$  coupling distributed so that

$$V_{\text{int}} = \sum_{j=1}^{2k} (-1)^j g^2 \phi^2 \chi_j^2 \quad (4.13)$$

and  $f_j = f, j = 1 \dots 2k$ . In order that the potential be strictly positive, it requires

$$\left( \frac{\lambda}{24} + \frac{Nf}{24} - \frac{Ng^2}{4} \right) > 0, \quad (4.14)$$

which for large  $N$  implies  $g^2 < f/6$ . In the alternating sign regime (ASR) the thermal masses are

$$m_T^2 \approx \frac{\lambda}{24} T^2 \quad (4.15)$$

and

$$\mu_T^2 \approx \frac{f}{24} T^2. \quad (4.16)$$

Following an analysis similar to above and for case 3 ( $\lambda_T \sim g^4$ ), we find a solution regime within the perturbative amplitude expansion,  $g\phi < \mu_T$ ,  $\lambda\phi < T$ , for  $g^2 < f^{3/2} \ln(2\sqrt{24/f})/46$  and  $N \sim 1/g^4$ . For example, these conditions are satisfied for  $f \lesssim 1.0$ ,  $g^2 \lesssim 1/20$ . In this example  $\lambda \sim g^2$ , but this can be modified in several ways. In general, when the  $\phi - \chi$  couplings are distributed between positive and negative strengths, it controls the growth

of  $m_T$  due to the cancellation of thermal mass contributions from the  $\chi$ -fields. Restricting the magnitude of  $m_T$ , in turn, increases the parameter regime and duration of overdamped motion. This example demonstrates another regime of overdamped motion in our model for small field amplitudes  $g^2\varphi_c^2 < \mu_T^2$ .

## B. Summing up the whole 1-loop series - The effective potential

The fact that overdamping in (3.7) for much of the parameter space demands large field amplitudes, at least within the approximation scheme used here, is a direct consequence of having a field dependent dissipation  $\eta(\varphi) \sim \varphi^2$ . Since in (2.7) we are considering a perturbative expansion for the 1-loop effective action in the field amplitudes (that is, in powers of  $\lambda\varphi_c^2/2$  and  $g_j^2\varphi_c^2$ ), the need for large field amplitudes may place doubts on the validity of our calculations for a considerable portion of the parameter space. Below we address this issue in two different ways; first by comparing our results with an improved one-loop approximation and then by using the subcritical bubbles method [30] to test the validity of the effective potential for large-amplitude fluctuations.

We start by computing the analog of (4.4) in the context of the whole one-loop approximation, *i.e.*, when  $\lambda\varphi_c^2/2$  and  $g_j^2\varphi_c^2$  in (2.6) are taken as part of field-dependent masses. For this, let us give an alternative computation of the evolution equation for  $\varphi_c$  in terms of the tadpole method of Weinberg [13,33,34]: in the shifting of the scalar field,  $\phi = \varphi_c + \eta$ , the requirement  $\langle \eta \rangle = 0$  leads, at the one-loop order, to the evolution equation for  $\varphi_c$  (for homogeneous fields)

$$\ddot{\varphi}_c + m^2\varphi_c + \frac{\lambda}{6}\varphi_c^3 + \frac{\lambda}{2}\varphi_c\langle\eta^2\rangle + \sum_j g_j^2\varphi_c\langle\chi_j^2\rangle = 0, \quad (4.17)$$

where  $\langle\eta^2\rangle$  and  $\langle\chi_j^2\rangle$  are given in terms of the coincidence limit of the (causal) two-point Green's functions  $G_\phi^{++}(x, x')$  and  $G_{\chi_j}^{++}(x, x')$ , respectively, which satisfy, in the fully dressed propagator form (see, e.g., Ringwald in [34])

$$\left[ \square + m^2 + \frac{\lambda}{2}\varphi_c^2 \right] G_\phi^{++}(x, x') + \int d^4z \Sigma_\phi(x, z) G_\phi^{++}(z, x') = i\delta(x, x') \quad (4.18)$$

and

$$\left[\square + \mu_j^2 + g_j^2 \varphi_c^2\right] G_{\chi_j}^{++}(x, x') + \int d^4 z \Sigma_{\chi_j}(x, z) G_{\chi_j}^{++}(z, x') = i\delta(x, x') , \quad (4.19)$$

where, in (4.18) and (4.19),  $\Sigma_\phi(x, x')$  and  $\Sigma_{\chi_j}(x, x')$  are the (causal) self-energies for the  $\phi$  and  $\chi_j$  fields, respectively. By expressing  $\eta(x)$  and  $\chi_j(x)$  in terms of mode functions, we can then evaluate the averages in (4.17). An explicit expression can be obtained in the approximation (equivalent to the adiabatic approximation)  $\dot{\omega}_\phi(\varphi_c)/\omega_\phi^2(\varphi_c) \ll 1$  and  $\dot{\omega}_\chi(\varphi_c)/\omega_\chi^2(\varphi_c) \ll 1$ , for which there is a WKB solution for the mode functions of the fields. In this paper, however, we will not carry out this calculation. A detailed study of this, in the context of an expanding background and along the proposals made in the next section, will be presented in a forthcoming paper.

For now, we can present the result of this calculation, by using the simplest formulation proposed in [11], based on a relaxation-time approximation of the kinetic equation, for the calculation of the averages in (4.17). We can then show that the (ensemble averaged) evolution equation for  $\varphi_c(t)$  can be expressed, in the quasi-adiabatic approximation (hydrodynamical regime of [11]), by

$$\ddot{\varphi}_c + V'_{\text{eff}}(\varphi_c) + \eta_1 \varphi_c^2 \dot{\varphi}_c = 0 , \quad (4.20)$$

where  $V'_{\text{eff}}(\varphi_c) = \frac{\partial V_{\text{eff}}(\varphi_c)}{\partial \varphi_c}$ , is the field derivative of the 1-loop effective potential,

$$\begin{aligned} V'_{\text{eff}}(\varphi_c) = & m^2 \varphi_c + \frac{\lambda}{6} \varphi_c^3 + \frac{\lambda}{4} \varphi_c \int \frac{d^3 q}{(2\pi)^3} \frac{1 + 2n(\omega_\phi)}{\omega_\phi} \\ & + \sum_j \frac{g_j^2}{2} \varphi_c \int \frac{d^3 q}{(2\pi)^3} \frac{1 + 2n(\omega_{\chi_j})}{\omega_{\chi_j}} , \end{aligned} \quad (4.21)$$

where  $\omega_\phi^2 = \mathbf{q}^2 + m_T^2 + \frac{\lambda}{2} \varphi_c^2$  and  $\omega_{\chi_j}^2 = \mathbf{q}^2 + \mu_j^2(T) + g_j^2 \varphi_c^2$  are the field dependent frequencies, with masses given in terms of the thermal ones<sup>5</sup>, Eqs. (2.16) and (2.17). Also,  $\eta_1$  in (4.20)

---

<sup>5</sup>Note that this will lead to the daisy corrected effective potential. In particular, once the thermal masses are being introduced in the derivative of the effective potential, expressed in terms of one-loop tadpole graphs in the Weinberg method, it is well known that this method leads to a consistent finite temperature effective potential [35], with daisy graphs incorporated.



is the same as in (3.12), but now with the masses replaced by the field dependent ones.

In terms of (4.20), in the overdamping approximation, the condition (4.2) becomes

$$\left| \frac{V'_{\text{eff}}}{\eta_1 \varphi_c^3} \right| \ll \Gamma . \quad (4.22)$$

Using Eq. (4.22), in the high temperature approximation for the fields,  $m_\phi(T)/T, m_{\chi_j}(T)/T \ll 1$ , we can show that the results obtained earlier, in terms of the amplitude expansion for the effective action, for instance, the results expressed in Fig. 3 (with  $m_T$  replaced with the field dependent mass  $m_\phi(T)$ ), remain approximately the same, for the cases where  $\varphi_c \lesssim 2T$ . Thus, at least for these values of the field amplitude, higher order corrections do not add to the effective potential. In other words, at leading order in the high-temperature expansion, the field derivative of  $V_{\text{eff}}$  can be just expressed as in (4.4),  $V'_{\text{eff}} \sim m_T^2 \varphi_c + \lambda_T/6 \varphi_c^3$ .

We can also address the issue of high-amplitude fluctuations by adopting a method suggested in Ref. [31], where it was applied to test the validity of the 1-loop approximation to the electroweak effective potential. We note that the results from this approach are entirely consistent with nonperturbative computations based on lattice gauge theories performed by K. Kajantie *et al.* [32].

The interactions of the field  $\varphi$  with a thermal environment will promote fluctuations around the perturbative vacuum. The subcritical bubbles method models these fluctuations as unstable spherically-symmetric configurations with a distribution of sizes and amplitudes. For details see Refs. [30,31]. Using a distribution function for these configurations, it is possible to compute the RMS amplitude of the fluctuations [31],

$$\bar{\varphi}(T) = \sqrt{\langle \varphi^2 \rangle_T - \langle \varphi \rangle_T^2} , \quad (4.23)$$

where  $\langle \dots \rangle$  is the thermal average defined in Ref. [31]. For the effective potential of Eq. (4.4), we obtain,

$$\bar{\varphi}^2(T) \simeq \frac{1}{6} m_T T . \quad (4.24)$$

Since the perturbative approach for the computation of the effective potential relies on a saddle-point approximation to the partition function, it will only be valid for small-amplitude fluctuations about the perturbative vacuum. For potentials which exhibit spontaneous symmetry breaking, it is customary to choose the maximum amplitude to be at the inflection point,  $\varphi_{\max} \lesssim \varphi_{\inf}$ . Here, since we have a potential with positive-definite curvature, we will conservatively assume that the perturbative expansion is valid for fluctuations dominated by the quadratic term of the effective potential, that is, for

$$\varphi_{\max}^2 \lesssim 12 \frac{m_T^2}{\lambda_T} . \quad (4.25)$$

The condition for the validity of the 1-loop approximation for the effective potential is then written as

$$\bar{\varphi}^2(T) \leq \varphi_{\max}^2 . \quad (4.26)$$

It is straightforward to apply this condition to the 3 cases analysed above. Since case 3 is the one with a larger range of parameters satisfying the adiabatic condition, we use it as an illustration. From Eqs. (4.10) and (4.11), we can write Eq. (4.26), after dividing by  $T^2$ , as the inequality

$$[f(g, N)]^{1/2} > \frac{g^4}{144\sqrt{6}} , \quad (4.27)$$

where,  $f(g, N) \equiv 24m_T^2/T^2$ . This condition is easily satisfied for a large range of parameters. In particular, for  $\lambda = 0.5$ ,  $g = 0.3$ ,  $N = 25$ , which are values inside the region of parameters allowed for overdamping shown in Fig. 3c for  $\varphi_c \gtrsim 2T$ , we obtain,  $\bar{\varphi} \simeq 0.3T$  and  $\varphi_{\max} \simeq 16T$ , well within the range of validity of the small-amplitude approximation. We thus conclude that it is possible to attain the adiabatic limit of strong dissipation within the 1-loop approximation scheme adopted here.

## V. APPLYING STRONG DISSIPATION TO WARM INFLATION

The calculation in Secs. II-IV presented a microscopic quantum field theory model of strong dissipation in Minkowski spacetime. This section addresses the application of this

calculation to the cosmological warm inflation scenario. Although we will not present a detailed extension of our previous results to an expanding spacetime, we will argue that most of the modifications are quite straight-forward up to the requirements for the warm inflation scenario.

### A. Formulation

Consider the standard Friedmann cosmology with Robertson-Walker metric

$$ds^2 = dt^2 - R^2(t) \left[ \frac{dr^2}{1 - kr^2} + r^2 d\theta^2 + r^2 \sin^2 \theta d\phi^2 \right]. \quad (5.1)$$

We restrict our analysis to flat space,  $k = 0$ , and quasistatic de Sitter expansion,  $H \equiv \dot{R}/R \approx \text{const.}$  For notational convenience, the origin of cosmic time is defined as the beginning of our treatment. For this metric, the minimally coupled Lagrangian for the model in Eq. (2.1) is

$$\begin{aligned} L = & \int_V d^3 \mathbf{x} e^{3Ht} \left\{ \frac{1}{2} \left( (\partial_0 \phi(\mathbf{x}, t))^2 - (e^{-Ht} \nabla \phi(\mathbf{x}, t))^2 - m^2 \phi^2(\mathbf{x}, t) \right) - V(\phi(\mathbf{x}, t)) \right. \\ & + \sum_i \frac{1}{2} \left[ (\partial_0 \chi_i(\mathbf{x}, t))^2 - (e^{-Ht} \nabla \chi_i(\mathbf{x}, t))^2 - \mu_i^2 \chi_i^2(\mathbf{x}, t) - \frac{f_i}{12} \chi_i^4(\mathbf{x}, t) \right] \\ & \left. - \sum_i \frac{g_i^2}{2} \chi_i^2(\mathbf{x}, t) \phi^2(\mathbf{x}, t) \right\}. \end{aligned} \quad (5.2)$$

There exists an alternative derivation of the ensemble average of Eq. (3.7), which was presented for a single scalar field, as an intuitive argument in [11]. In the context of a single scalar field, the method is to work directly with the operator equation of motion for  $\phi(\mathbf{x}, t)$ . The operator  $\phi$  is reexpressed as the sum of a c-number  $\varphi_c(t)$ , representing the classical displacement, plus a shifted operator  $\eta(\mathbf{x}, t)$ ,

$$\phi(\mathbf{x}, t) = \varphi_c(t) + \eta(\mathbf{x}, t) \quad (5.3)$$

with  $\langle \phi(\mathbf{x}, t) \rangle_\beta = \varphi_c(t)$ . A thermal average is taken of this equation of motion, in which thermal expectation values involving  $\eta(\mathbf{x}, t)$  are computed such that  $\varphi_c(t)$  is treated as an adiabatic parameter. To the order of perturbation theory considered in the previous sections,

for the single scalar field the intuitive derivation in [11] gives the same effective equation of motion as the ensemble average of Eq. (3.7) as shown in [2].

No new considerations are needed to apply this intuitive derivation to the model in Eq. (2.1). The  $\chi_i(\mathbf{x}, t)$  fields are treated as quantum fluctuations similar to  $\eta(\mathbf{x}, t)$ . From the treatment in [11], it follows that the expressions for  $m_T$ ,  $\lambda_T$  and  $\eta_1$  in Eq. (3.7) will arise from the thermal averages,  $\langle \eta^2(\mathbf{x}, t) \rangle_\beta$  and  $\langle \chi_i^2(\mathbf{x}, t) \rangle_\beta$ , taken with respect to the instantaneous background  $\varphi_c(t)$ .

Although the approach in [11] immediately isolates the dissipative term and the finite temperature renormalizations at the level of the equation of motion, it is not systematic to all orders. Furthermore, it cannot treat noise and it is valid only in the adiabatic approximation. These limitations can be accounted for in the closed-time-path formalism used in this paper. A recent work [36] has discussed some of the difficulties associated with extending this formalism to an expanding background in order to treat noise and dissipation. Our goal at present is more modest. As an easier first step, the intuitive derivation of [11] is extended to an expanding background.

The exact operator equations of motion from the Lagrangian Eq. (5.2) are

$$\ddot{\phi}(\mathbf{x}, t) + 3H\dot{\phi}(\mathbf{x}, t) - e^{-2Ht}\nabla^2\phi(\mathbf{x}, t) + m^2\phi(\mathbf{x}, t) + \frac{\delta V}{\delta\phi(\mathbf{x}, t)} + \sum_i g_i^2\phi(\mathbf{x}, t)\chi^2(\mathbf{x}, t) = 0, \quad (5.4)$$

and

$$\ddot{\chi}_i(\mathbf{x}, t) + 3H\dot{\chi}_i(\mathbf{x}, t) - e^{-2Ht}\nabla^2\chi_i(\mathbf{x}, t) + g_i^2\chi_i(\mathbf{x}, t)\phi^2(\mathbf{x}, t) + \mu_i^2\chi_i(\mathbf{x}, t) + \frac{f_i}{6}\chi_i(\mathbf{x}, t)^3 = 0. \quad (5.5)$$

The objective is to displace the operator  $\phi(\mathbf{x}, t)$  by a  $\mathbf{x}$ -independent c-number at time  $t = 0$ ,  $\langle \phi(\mathbf{x}, t = 0) \rangle_\beta = \varphi_c(0)$ , and then determine the evolution of the expectation value  $\langle \phi(\mathbf{x}, t) \rangle_\beta \equiv \varphi_c(t)$  by solving Eqs. (5.4) and (5.5) perturbatively. Thus  $\phi(\mathbf{x}, t)$  is reexpressed as Eq. (5.3). With this definition of  $\varphi_c(t)$ , for flat,  $k = 0$ , nonexpanding,  $H = 0$ , spacetime, the resulting equation of motion is the same as the ensemble average of the equation of motion, Eq. (3.7).

For the case of expanding spacetime,  $H \neq 0$ , in order to obtain the equation of motion for  $\varphi_c(t)$ , thermal expectation values must be taken of Eqs. (5.4) and (5.5). Provided the temperature,  $1/\beta$ , of the thermal bath is time independent, (*i.e.*, rapid equilibration time scales), thermal expectation values of terms linear in  $\phi(\mathbf{x}, t)$  can be replaced by  $\varphi_c(t)$ , just as for the nonexpanding case. In evaluating  $\langle \eta^2(\mathbf{x}, t) \rangle_\beta$  and  $\langle \chi_i^2(\mathbf{x}, t) \rangle_\beta$ , if the characteristic time scale for the quantum fluctuations is much faster than the expansion time scale,  $1/H$ , the calculation is no different from the Minkowski space situation. This criteria is self-consistently satisfied provided

$$\Gamma_\chi, \Gamma_\phi \gg H, \quad (5.6)$$

where the left hand side is given in Eqs. (2.14) and (2.15) for our model.

These arguments suggest that at leading nontrivial order, the effective equation of motion for  $\varphi_c(t)$  in an expanding de Sitter spacetime, under the same conditions required for Eq. (3.7) plus the additional condition Eq. (5.6) is

$$\ddot{\varphi}_c(t) + [\eta_1 \varphi_c^2(t) + 3H] \dot{\varphi}_c(t) + m_T^2 \varphi_c(t) + \frac{\lambda_T}{6} \varphi_c^3(t) = 0. \quad (5.7)$$

Further justification that Eq. (5.7) is the appropriate replacement of Eq. (3.7), for expanding de Sitter space, can be obtained from [6], where an effective equation of motion similar to Eq. (5.7) was obtained for a model like Eq. (5.2). However, the coupling between fields was linear,  $\phi \chi_i$ , which is analytically much more tractable than the present case of quadratic coupling,  $\phi^2 \chi_i^2$ .

The entire discussion above assumes that the temperature has a well defined meaning in an expanding background. Furthermore, Eq. (5.7) has been motivated under the restriction Eq. (5.6). As will be discussed next, condition (5.6) is a specific example of a general microscopic property argued in [6] to be a necessary condition for warm inflation. As such, when (5.7) is applied to the warm inflation scenario, condition (5.6) imposes no additional restriction.

The warm inflation picture requires that an order parameter, in a strongly dissipative regime, slowly rolls down a potential, liberating vacuum energy into radiation energy,  $\rho_r$ . The

nonisentropic expansion which underlies warm inflation imposes that the rate of radiation production is sufficient to compensate for red-shift losses due to cosmological expansion,

$$H \gg \frac{|\dot{\rho}_r|}{\rho_r}. \quad (5.8)$$

To give meaning to temperature, the newly liberated radiation must thermalize at a scale  $\Gamma_{\text{rad}}$  which is faster than the expansion scale,

$$\Gamma_{\text{rad}} \gg H. \quad (5.9)$$

Minimally this requires an energy transfer rate from vacuum to radiation that is faster than the expansion rate, which in our model implies the condition (5.6). Thus, Eq. (5.9) is necessary to justify a temperature parameter  $T$ , which, combined with condition (5.6), are sufficient to justify the arguments leading to Eq. (5.7). To completely justify a temperature parameter for an expanding background spacetime, it is required studying the thermalization of the radiation, once it is liberated. General arguments, as well as specific calculations [37,38] at high temperature, indicate that this rate is set by the temperature  $\Gamma_{\text{rad}} \sim \alpha T$ , for some appropriate, model dependent, coefficient  $\alpha$ . This minimally requires  $T \gg H$ . However,  $\alpha$  may be very small, as for example in Eqs. (2.14) and (2.15). Thus the correct constraint is

$$\alpha T \gg H. \quad (5.10)$$

This problem will not be considered further here. Eq. (5.6) will be our only criteria for thermalization. This is equivalent to assuming that the thermalization rate is at least as fast as the energy transfer rate.

Once Eq. (5.7) is accepted as the macroscopic equation governing the evolution of the order parameter  $\varphi_c(t)$ , it can be used as a given input to construct warm inflation scenarios as in [7,9]. The microscopic origin of the equation can be forgotten up to restrictions on parameters and the self consistency condition Eq. (5.6). For a general equation like Eq. (5.7), the warm inflation scenario requires the strong dissipative regime [7]:

$$[\eta(\varphi_c) + 3H] \dot{\varphi}_c \gg \ddot{\varphi}_c, \quad (5.11)$$

with  $\eta(\varphi_c) = \eta_1 \varphi_c^2$  for our model. For the derivation in Secs. II-IV, where  $H = 0$ , this condition is sufficient to satisfy the adiabatic condition, Eq. (4.2), which is required for the consistency of the microscopic calculation. As such, this model provides an example of a general point conveyed in [6], that warm inflation defines a good regime for application of finite temperature dissipative quantum field theory methods. The study of warm inflation in [6,7,9] also found that to satisfy observational constraints on the expansion factor, it requires

$$\eta(\varphi_c) \gg 3H. \quad (5.12)$$

Thus, warm inflation is an extreme example of dissipative dynamic during de Sitter expansion. As demonstrated in [8,39], dissipation is generally prevalent during inflation. The microscopic model in this paper could be used to examine the general case, but then the condition (5.12) can be relaxed. Here, only the warm inflation regime will be further examined. Thus in the limit given by Eq. (5.12) and based on the remaining discussion in this section, the equation of motion for the order parameter  $\varphi_c(t)$  in our model for the warm inflation scenario turns out to be Eq. (4.4) but with the additional constraint Eq. (5.6).

The other input for constructing warm inflation scenarios is the free energy in the expanding environment for the model (5.2). It already has been argued above that temperature is a good parameter for describing the state of the radiation in the warm inflation regime. It also follows from the above that the change in temperature can be treated adiabatically in the thermodynamic functions, since this requires  $\Gamma_{\text{rad}} \gg \dot{T}/T$ , which is automatically satisfied due to Eq. (5.9). Therefore the free energy density should be well represented by the Minkowski space expression, with temperature treated as an adiabatic parameter. For the model in Secs. II-IV, the free energy density is

$$F(\varphi_c, T) = \frac{m_T^2}{2} \varphi_c^2 + \frac{\lambda_T}{24} \varphi_c^4 - \frac{(N+1)\pi^2}{90} T^4, \quad (5.13)$$

where the factor  $N+1$ , in the last term, comes from the functional integration over the  $\chi$  fields and the  $\phi$ -field's fluctuations. Having established this to be the free energy density

for the warm inflation scenario, the other thermodynamic functions such as pressure, energy density and entropy density can be easily obtained.

With the free energy (5.13) and the order parameter equation of motion, Eq. (5.7), determined, the time evolution of the three unknowns: temperature  $T(t)$ , scale factor  $R(t)$  and order parameter  $\varphi_c(t)$ , can be obtained from Eq. (5.7) plus any two independent equations from Friedmann cosmology along with a self consistency check for adiabaticity, Eq. (5.11). At this point the procedure in [9] can be followed. However due to the microscopic origin of this model, additional self consistency checks are necessary for adiabaticity, given by Eq. (4.2) and thermalization, Eq. (5.6). Observationally interesting expansion factors will require  $H > \dot{\phi}/\phi$ , in which case the condition (5.6) immediately implies the microscopic adiabatic condition (4.2).

## B. Results

Up to this point, the formulation of warm inflation in conjunction with a microscopic dynamics has been general. In the remainder of this section, some demonstrative calculations of this cosmology will be presented based on our microscopic model. An exhaustive analysis of the parameter space will not be performed. In this first examination, the emphasis is to understand the interplay between the microscopic and macroscopic physics of warm inflation for generic potentials, which in particular, have curvature scale of order the temperature scale. For such potentials, thermal fluctuations that displace  $\varphi_c(0)$  substantially from the origin are exponentially suppressed. However, it is such fluctuations that allow enough time, during the roll down back to the origin, for the universe to inflate sufficiently. As such, this elementary fact, in any case, quells significant interest in comparing the cases we will examine to observation.

It should be noted that the order parameter in this symmetry restored warm inflation regime is configured similar to those in the chaotic inflation scenario [40]. However, in the chaotic inflation scenario the potentials are ultra-flat. Such potentials permit large fluctu-



ations of the order parameter and in fact prefer them. The dissipative model in this paper could be studied for the case of ultra-flat potentials, perhaps motivated by supersymmetric model building. This would extend the pure quantum mechanical, new-inflation type dynamics of chaotic inflation into the intermediate regime discussed in [8,39]. This will not be examined here.

Proceeding with our demonstrative examination of warm inflation, let the origin of time be the beginning of the inflationlike regime (BI) and also the beginning of our treatment. The basic picture of the particular warm inflation scenario studied here is as follows. At  $t = 0$  the initial conditions are arranged so that the field is displaced from the origin  $\langle\phi(0)\rangle = \phi_{BI}$ , the temperature of the universe is  $T_{BI}$  and since the universe is at the onset of the inflation-like regime, by definition this means the vacuum energy density equals the radiation energy density,  $\rho_v(0) = \rho_r(0)$ . For  $t > 0$  the field will relax back to the origin within a strongly dissipative regime and in the process liberate vacuum energy into radiation energy. Simultaneously, the scale factor will undergo inflation-like expansion. During the roll-down period, the vacuum energy first dominates until at some point it is superseded by the radiation energy. At this point the universe smoothly exits the inflation-like regime into the radiation dominated regime.

From our model in the previous sections, we will consider the case of  $N'$   $\chi$ -bosons ( $\chi'$ ) with  $g_j = g \gg f_j, j = 1 \dots N'$  and  $N - N'$   $\chi$ -bosons ( $\chi$ ) with  $g_j \ll f_j = f, j = N' + 1 \dots N$ . For this model, the dissipative dynamics of  $\varphi_c$ , expressed through  $m_T, \lambda_T$  and  $\eta_1$ , is controlled by the  $N'$   $\chi$ -bosons. The other  $N - N'$   $\chi$ -bosons only serve as additional fields in the radiation bath. For this purpose, from Eq. (2.15), for  $f \geq g^2$  the  $\chi$  and  $\chi'$  bosons will be equally effective in thermalizing the radiation energy.

In this paper we will examine this scenario in the regime

$$\frac{\lambda_T \varphi_c^4}{24} \gg \frac{m_T^2 \varphi_c^2}{2}. \quad (5.14)$$

and in the high temperature limit  $T \gg m_T, \mu_T$ . Also, for ease of presentation, we will write the expression for  $\Gamma(q)$  at  $\mathbf{q} = 0$ . Although with these simplifications the results will not be

cosmologically interesting, it is a good example to demonstrate the general procedure. In this regime, the effective equation of motion for  $\varphi_c$ , from Eq. (4.4), is:

$$\frac{d\varphi_c}{dt} = -\frac{B_2}{4}\varphi_c, \quad (5.15)$$

where

$$B_2 \equiv \frac{2\lambda_T}{3\eta_1} \approx \frac{\pi T_{BI}\lambda_T}{72N'\ln(2T_{BI}/\mu_{T_{BI}})}. \quad (5.16)$$

Formally the Friedmann cosmology for the warm inflation scenario associated with the above equation was called the quadratic limit in [9].

The macroscopic and microscopic requirements of warm inflation will imply various parametric constraints which are as follows. Eq. (5.14) will be satisfied by requiring:

$$\frac{\lambda_T\varphi_{BI}^4}{24} = r\frac{m_T^2\varphi_{BI}^2}{2}, \quad (5.17)$$

where the parameter  $r \gg 1$  has been introduced. As shown in [9], throughout the inflation-like period until just before it ends, the temperature drops slightly faster than  $\phi$ . As such, the thermal mass term,  $m_T^2\phi^2/2 \sim T^2\phi^2$ , will continue to satisfy Eq. (5.14) given that initially it does.

The number of e-folds,  $N_e$  obtained during the roll-down is, from [9],

$$N_e \approx \frac{2H}{B_2}, \quad (5.18)$$

where

$$H = \sqrt{\frac{8\pi\lambda_T\varphi_{BI}^4}{72m_p^2}}, \quad (5.19)$$

with  $m_p$  the Planck mass. The microscopic condition, Eq. (5.6), requires

$$\frac{g^4T}{192\pi} \gg \frac{\sqrt{\pi\lambda_T}\varphi_{BI}^2}{3m_p}. \quad (5.20)$$

The threshold condition for inflation,  $\rho_v(0) = \rho_r(0)$ , implies

$$\frac{(N+1)\pi^2}{30}T_{BI}^4 = \frac{\lambda_T\varphi_{BI}^4}{24}. \quad (5.21)$$

Finally, the validity of the perturbative derivation in the previous sections will require

$$g, \lambda, \frac{m_T}{T}, \lambda_T < 1, \quad (5.22)$$

where  $m_T^2 \sim (\lambda + 2N'g^2)T^2/24$  and  $\lambda_T \approx \lambda - \frac{3\sqrt{3}}{2\pi}N'g^3$ .

Eq. (5.20) can be turned into an equality, in which case, along with Eqs. (5.17), (5.18), and (5.21), they determine the boundary of the allowed parameter space. Thus there are six constraining equations for the eleven quantities  $\lambda, g, \lambda_T, m_T, m_p, \varphi_{BI}, N, N', N_e, r$ , and  $T_{BI}$ . We will let  $T_{BI}$  set the overall scale and will fix  $N', N_e, r, g$ . Then, based on the constraint equations, this determines the remaining parameters. In particular, we have for  $\lambda_T$ :

$$\lambda_T \approx \frac{3N'g^4 \ln(2\sqrt{12}/g)}{4N_e\pi^2}. \quad (5.23)$$

This expression is suggestive of the case 3 analyzed in Sec. IV. For such, taking then  $m_T^2 \sim (3g\sqrt{3}/2\pi + 2)N'g^2T^2/24$ , we get the additional parameters:

$$\varphi_{BI} \approx \frac{2\pi T_{BI}}{g} \sqrt{\frac{(3g\sqrt{3}/2\pi + 2)N_e r}{6 \ln(2\sqrt{12}/g)}}, \quad (5.24)$$

$$N + 1 \approx \frac{5r^2 N' N_e}{12 \ln(2\sqrt{12}/g)} \left( \frac{3\sqrt{3}}{2\pi}g + 2 \right)^2, \quad (5.25)$$

and

$$m_p \approx \frac{192\pi^2 r T_{BI}}{9g^4} \left( \frac{3\sqrt{3}}{2\pi}g + 2 \right) \sqrt{\frac{3\pi N' N_e}{\ln(2\sqrt{12}/g)}}. \quad (5.26)$$

Based on these equations, it is not difficult to find parametric regimes in which the warm inflation scenario is realized, but it is only for  $N_e < 1$ . As such, this simple case has no observational relevance. There are a few improvements that could be made to our analysis that would increase  $N_e$ . Firstly our estimates above ignore the effects of the thermal mass term,  $m_T^2\varphi_c^2/2$ , on the dynamics. Its contribution to the energy density and pressure are  $\rho_{m_T} = -m_T^2\varphi_c^2/2$  and  $p_{m_T} = \rho_{m_T}$  respectively. Thus it helps the  $\varphi_c^4$  term to drive inflation. Secondly, recall that the dissipative coefficient  $\eta_1 \sim 1/T$ . In the above analysis, we fixed

$T = T_{BI}$ . However, during the roll-down, temperature does fall by a factor of order ten, which in turn would increase  $\eta_1$ . Finally the parameter regime could be extended to include both positive and negative  $\phi - \chi$  couplings, such as the ASR case described in subsection IV.A. As noted there, in this regime the duration of overdamped motion can be increased significantly within the perturbative amplitude expansion. This directly corresponds to increasing the e-folds  $N_e$ .

A more elementary modification is to extend the region of validity to larger displacements of  $\varphi_c$ . The extension to this larger regime can be treated by a summation of the complete one-loop series as outlined in subsection IV.B. Overdamped motion for much larger displacements of  $\varphi_c$  can also be attained by a modification to the  $\phi - \chi$  interaction in Eq. (2.1) as

$$\sum_{j=1}^N \frac{g^2}{2} \phi^2 \chi_j^2 \rightarrow \sum_{j=1}^N \frac{g^2}{2} (\phi - M_j)^2 \chi_j^2. \quad (5.27)$$

In this distributed mass model (DMM), a given  $\chi_j$ -field is thermally excited when its effective mass  $g^2(\varphi_c - M_j)^2 < T^2$ . The contribution from the thermally excited  $\chi$ -fields to the effective dynamics of  $\varphi_c$  is similar to our calculations in sections II-IV. As such, an effective equation of motion similar to Eq. (4.4) can be obtained for this modified model. Given an appropriate distribution of mass coefficients  $M_j$  along the path of  $\varphi_c$ , from an arbitrarily large initial displacement  $\varphi_{BI}$ ,  $\varphi_c(t)$  could undergo overdamped motion along its entire path. Details will be presented elsewhere on the warm inflation scenario which considers these various cases.

For this “symmetry restored” case, initial fluctuations of  $\varphi_c(t)$ ,  $\varphi_{BI}$ , are strongly suppressed with probability  $\exp(-\text{volume } \rho/T_{BI}) \sim \exp[-(128\pi)^3 N N_e r^2/g^{12}]$ , where the volume  $\sim 1/H^3$ . The most optimistic initial conditions have probability  $\sim \exp[-1 \times 10^7]$ . Thus, unless a viable mechanism is found to justify a large enough initial value of  $\varphi_c$ , the regime investigated here may not be very relevant for practical applications of warm inflation. In any case, the microscopic dynamics of the symmetry restored regime investigated here is similar to more realistic scenarios in the symmetry broken regime, where the field has an average initial value close or identical to zero. An important difference being that the initial

state in the latter case has no Boltzmann suppression.

This section has made an initial examination of treating strong dissipation from first principles during a de Sitter expansion regime. Further results will be presented elsewhere as well as a calculation similar to this one, for the symmetry broken case.

## VI. CONCLUSION

In this paper a microscopic quantum field theory model has been presented, describing overdamped motion of a scalar field. Commonly, such behavior is treated phenomenologically by Ginzburg-Landau order parameter kinetics. Our model provides a first principle explanation of how kinetics equivalent to the Ginzburg-Landau type, which is first order in time, arise for inherently second order dynamical systems. The microscopic treatment of this problem, in principle, should be well controlled, due to its fundamental reliance on the adiabatic limit, and our model exemplifies this expectation.

The calculational method for treating dissipation in this paper has one distinct difference from several other related works. In our calculation, we consider the effect of particle lifetimes in the effective equation of motion. To our knowledge, this effect has been discussed in only a few works in the past [2,11,14].

Secs. II-IV presented a general, flat-space treatment, which offers a microscopic justification to the often used limit of diffusive Ginzburg-Landau scalar field dynamics. We have shown how it is possible to obtain an effective evolution for the scalar field which is first-order in time, due to its own thermal dissipation effects, interpreted microscopically as its decay into many quanta. In a sense, the field acts as its own brakes, the slowing of its dynamics being attributed to the highly viscous medium where it propagates, a densely populated sea of its own decay products.

The application that we considered in Sec. V was in expanding spacetime, for the cosmological warm inflation scenario. Although we did not formally derive the extension of our flat-space model of Secs. II-IV to an expanding background, we did present heuristic

arguments that validate this extension for the special needs of warm inflation. The results of the simple analysis in Sec. V are strongly dependent on initial conditions and may be difficult to implement for models of observational interest. Nevertheless, these results will provide useful guidance both for modifications of this model and for our next study of the symmetry broken regime.

The direct significance of the present study to inflationary cosmology would be to the initial state problem [41] in scenarios during symmetry breaking. The initial conditions required for warm inflation in the symmetry broken case are similar to new inflation. The requirement is a thermalized inflaton field, which at the onset of the warm inflation regime is homogeneous with expectation value  $\langle\phi\rangle_\beta = 0$ . Although we have made no detailed application of our results to this problem, some general features are evident from the analysis in Sec. V. In particular, both the suppression of large fluctuations and thermalization are mutually consistent with strong dissipative dynamics. Many of the difficulties that have been discussed [41,42] in association with the initial state problem, are eliminated in the strong dissipative regime. In addition, the damping of fluctuations should simplify the formal problem of coupling this model to classical gravity. Thus, the strong dissipative regime appears to have the correct features both to carry the universe into an inflation-like phase and then to smoothly exit into a hot big-bang regime.

## ACKNOWLEDGMENTS

We thank R. Holman for helpful discussions. AB was supported by a Department of Energy grant. MG was partially supported at Dartmouth College by the National Science Foundation through a Presidential Faculty Fellows Award no. PHY-9453431 and by the National Aeronautics and Space Administration grant no. NAGW-4270. MG thanks both Fermilab and the Osservatorio di Roma for their kind hospitality during the completion of this work. ROR was partially supported by Fundação de Amparo à Pesquisa no Estado do Rio de Janeiro - FAPERJ and by Conselho Nacional de Desenvolvimento Científico e

## APPENDIX A:

We now give a brief overview of the calculation of the imaginary part of the two-loop, setting sun, self-energy terms in (2.10) and (2.11). Let us express generically those diagrams in terms of field propagators with masses  $m_s$  and  $m_t$  and external lines of type  $s$ . For an interaction between  $s$  and  $t$  fields of the form  $g_{s,t}^2/2 s^2 t^2$  (for  $s = t = \phi$  ( $\chi_j$ ),  $g_{s,t}^2 = \lambda/12$  ( $f_j/12$ ) and for  $s = \phi$ ,  $t = \chi_j$ ,  $g_{s,t}^2 = g_j^2$ ) the imaginary part of the two-loop sunset diagram for the  $s$  field can be expressed by (see for example, in Ref. [21], Appendix G and also Wang and Heinz in [22]):

$$\begin{aligned}
 \text{Im}\Sigma_s(q) &= \text{Im} \left[ \text{---} \bigcirc \text{---} \right] = \\
 &= S_{s,t} g_{s,t}^4 \left(1 - e^{-\beta E_q^s}\right) \sum_{\sigma=\pm 1} \sigma_{k+q} \sigma_l \sigma_{k+l} \frac{1}{8(2\pi)^5} \int \frac{d^3 k d^3 l}{E_l^t E_{k+q}^s E_{k+l}^t} \left[1 + n(\sigma_{k+q} E_{k+q}^s)\right] \\
 &\times \left[1 + n(\sigma_l E_l^t)\right] \left[1 + n(\sigma_{k+l} E_{k+l}^t)\right] \delta(E_q^s - \sigma_l E_l^t - \sigma_{k+q} E_{k+q}^s - \sigma_{k+l} E_{k+l}^t), \tag{A1}
 \end{aligned}$$

where  $E_k^s = \sqrt{\mathbf{k}^2 + m_s^2}$ ,  $n(E)$  is the bose-distribution function and  $S_{s,t}$  is a symmetry factor: for  $s = t$ ,  $S = 12$  and for  $s \neq t$ ,  $S = 1$ . By expanding in the sum in  $\sigma$  and retaining only the on-shell, energy conserving processes (corresponding to the scattering processes  $st \rightarrow st$ ,  $ts \rightarrow ts$ ), we obtain the result:

$$\begin{aligned}
 \text{Im}\Sigma_s(q) &= S_{s,t} g_{s,t}^4 \frac{\left(1 + \frac{1}{2} \delta_{s,t}\right)}{4(2\pi)^5} \left(1 - e^{-\beta E_q^s}\right) \int \frac{d^3 k d^3 l}{E_l^t E_{k+q}^s E_{k+l}^t} \left[1 + n(E_{k+q}^s)\right] \left[1 + n(E_l^t)\right] n(E_{k+l}^t) \\
 &\times \delta(E_q^s - E_l^t - E_{k+q}^s + E_{k+l}^t), \tag{A2}
 \end{aligned}$$

with  $\delta_{s,t} = 1$  for  $m_s = m_t$  and  $\delta_{s,t} = 0$  for  $m_s \neq m_t$ .  $\text{Im}\Sigma(q)$  for  $s = t$  has been obtained in details in Refs. [21] and [22]. In particular, Wand and Heinz in [22] have discussed and obtained in detail the kinematic limits, for the  $\lambda\phi^4$  model, of the integration on the momenta in (A2), implicit in the Dirac delta-function. Here we obtain the results for the

case of  $m_s \neq m_t$ . In (A2), by defining in the three-dimensional momentum integrations the angular differentials  $d(\cos \theta_k) = dE_{k+q}^s E_{k+q}^s / (kq)$  and  $d(\cos \theta_l) = dE_{k+l}^t E_{k+l}^t / (kl)$  ( $k, q, l = |\mathbf{k}|, |\mathbf{q}|, |\mathbf{l}|$ ), we are then able to perform the angular integrals in (A2). From the constraint in the integration limits for  $k$  and  $l$ , which comes from the delta-function, we obtain the following result for  $\text{Im}\Sigma_s(q)$ ,

$$\begin{aligned} \text{Im}\Sigma_s(q) = & S_{s,t} g_{s,t}^4 \frac{T \left(1 + \frac{1}{2}\delta_{s,t}\right)}{4(2\pi)^3 q} \left(1 - e^{-\beta E_q^s}\right) \left\{ \int_0^\infty dk \int_{-u(k,q)}^{u(-k,q)} \frac{ldl}{E_l^t} \left[1 + n(E_q^s - E_l^t)\right] \left[1 + n(E_l^t)\right] \right. \\ & \times \ln \left( \frac{e^{\beta E_{k+l}^t} - 1}{e^{\beta E_{k+l}^t} - e^{\beta(E_l^t - E_q^s)}} \right) + \left( \int_{-q}^\infty dk \int_{u(k+q,q)}^\infty \frac{ldl}{E_l^t} - \int_q^\infty dk \int_{u(-k+q,q)}^\infty \frac{ldl}{E_l^t} \right) \\ & \times \left[1 + n(E_q^s - E_l^t)\right] \left[1 + n(E_l^t)\right] \ln \left( \frac{e^{\beta E_k^s} - 1}{e^{\beta E_k^s} - e^{\beta(E_q^s - E_l^t)}} \right) \Big\}, \end{aligned} \quad (\text{A3})$$

where, in the above expressions, the function  $u(k, q)$  is given by

$$\begin{aligned} u(k, q) = & \frac{1}{2} \left\{ k - \frac{1}{km_s} \left[ \sqrt{(k-q)^2 + m_s^2} - \sqrt{q^2 + m_s^2} \right] \left( k^2 m_s^2 + 2m_s^2 m_t^2 + 2q^2 m_t^2 \right. \right. \\ & \left. \left. - 2kqm_t^2 + 2m_t^2 \sqrt{(k-q)^2 + m_s^2} \sqrt{q^2 + m_s^2} \right)^{\frac{1}{2}} \right\}. \end{aligned} \quad (\text{A4})$$

In the first term of (A3), we can make the change of integration variables  $k+l = k'$ ,  $l = l'$ , to obtain  $l' dl' / E_{l'}^t = dE_{l'}^t$ . Doing the same for the remaining integrals,  $ldl / E_l^t = dE_l^t$ , relabeling  $l'$  and  $k'$  back to  $l$ ,  $k$ , and performing a new change of integration variables,  $y = e^{-\beta E_l^t}$ ,  $dy = -\beta e^{-\beta E_l^t} dE_l^t$ , we are able to compute the  $y$  integrations. From this point on, the integrations are equivalent to the ones in [21], once we change the integration limits in the  $k$  and  $l$  integrals, and take into account the function  $u(k, q)$ , Eq. (A4). The results shown in Sec. II for  $\Gamma_\phi$ ,  $\Gamma_{\chi_j}$ , Eqs. (2.14) and (2.15), are obtained once the limit of vanishing  $q$  ( $|\mathbf{q}| = 0$ ), is taken in the above equations.

## APPENDIX B:

Let us now compute the expression on the LHS of (3.5) in the adiabatic approximation, stressing the need for regularizing the propagators with quasi-particle lifetimes. Let us write the LHS of (3.5) in terms of the adiabatic series:



$$\begin{aligned}
& \int d^4x' \varphi_c^2(x') \text{Im} \left[ G^{++} \right]_{\mathbf{x}, \mathbf{x}'}^2 \theta(t - t') \\
&= \sum_n \int d^3x' \int \frac{d^3k}{(2\pi)^3} e^{i\mathbf{k} \cdot (\mathbf{x} - \mathbf{x}')} \frac{1}{n!} \left. \frac{\partial^n (\varphi_c^2)}{\partial t'^n} \right|_{t'=t} \int \frac{d^3q}{(2\pi)^3} \int_{-\infty}^t dt' (t' - t)^n \\
&\times \text{Im} \left[ G^{++}(\mathbf{q}, |t - t'|) G^{++}(\mathbf{q} - \mathbf{k}, |t - t'|) \right] , \tag{B1}
\end{aligned}$$

where  $G^{++}(\mathbf{q}, t - t')$  can be read from (2.20) and (2.21) and it refers generically to the  $\phi$  or  $\chi_j$  field propagators. The approximation of considering a homogeneous field,  $\varphi_c \equiv \varphi_c(t)$ , is equivalent to taking the limit  $\mathbf{k} \rightarrow 0$  for the external momentum in  $G^{++}(\mathbf{q} - \mathbf{k}, |t - t'|)$ . In this case the  $x'$  and  $k$  integrations in (B1) can be done trivially. However, it is known that taking the limit of zero external momentum ( $k_\mu \rightarrow 0$ ) [43,44] in self-energy expressions, which are given in terms of products of non-local propagators, can be problematic. This is related to the non-analyticity of these expressions around the origin. In particular, Gross, Pisarski, and Yaffe in [43] argue that a correct way of taking the limit  $k_\mu \rightarrow 0$ , at finite temperatures, is to first take  $k_0 \rightarrow 0$  and then  $\mathbf{k} \rightarrow 0$ . They also argue that the non-analyticity problem, which comes from a failure to do a self-consistent calculation, would be eliminated once fully-dressed propagators are taken consistently into account. We note, in particular, that for fully-dressed propagators the decay width  $\Gamma$  works as a regulator.

In (B1), the limit  $k_0 \rightarrow 0$  is implicit in the adiabatic approximation, where the fields are required to change slowly in time, while the limit  $\mathbf{k} \rightarrow 0$  is implemented by approximating the fields to be homogeneous. In evaluating (B1), we will first compute the time integral, expand in terms of the “regulator”  $\Gamma$ , and then finally take the limit  $\mathbf{k} \rightarrow 0$ . This is the opposite of what was done in obtaining Eq. (3.5). From this lesson we will see both the importance of considering fully-dressed propagators and how consistent results can be obtained once the limits are taken in the correct order. This will be crucial when evaluating the dissipation contribution ( $n = 1$ , in (B1)).

Consider the time integral on the RHS of Eq. (B1) and expand it to first order in the “regulator”,  $\Gamma$  (which is of order  $\lambda^2, g^4$ ). Higher order terms in  $\Gamma$  need to be considered in conjunction with higher order loop terms, for consistency. For  $n = 0$ , the zeroth-order in the adiabatic approximation, we obtain

$$\begin{aligned}
& \int_{-\infty}^t dt' \text{Im} \left[ G^{++}(\mathbf{q}, |t-t'|) G^{++}(\mathbf{q}-\mathbf{k}, |t-t'|) \right] \\
& \simeq \frac{1}{4\omega_{\mathbf{q}}\omega_{\mathbf{q}-\mathbf{k}}} \left[ -\frac{1}{\omega_{\mathbf{q}} + \omega_{\mathbf{q}-\mathbf{k}}} + 2 \frac{\omega_{\mathbf{q}-\mathbf{k}} n(\omega_{\mathbf{q}}) - \omega_{\mathbf{q}} n(\omega_{\mathbf{q}-\mathbf{k}})}{\omega_{\mathbf{q}}^2 - \omega_{\mathbf{q}-\mathbf{k}}^2} \right] + \mathcal{O} \left[ \left( \frac{\Gamma_{\mathbf{q}} + \Gamma_{\mathbf{q}-\mathbf{k}}}{\omega_{\mathbf{q}} + \omega_{\mathbf{q}-\mathbf{k}}} \right)^2 \right]. \quad (\text{B2})
\end{aligned}$$

Taking the limit  $\mathbf{k} \rightarrow 0$ , we obtain

$$\lim_{\mathbf{k} \rightarrow 0} \int_{-\infty}^t dt' \text{Im} \left[ G^{++}(\mathbf{q}, |t-t'|) G^{++}(\mathbf{q}-\mathbf{k}, |t-t'|) \right] \rightarrow -\frac{[1 + 2n(\omega_{\mathbf{q}})]}{8\omega_{\mathbf{q}}^3} - \beta \frac{n(\omega_{\mathbf{q}}) [1 + n(\omega_{\mathbf{q}})]}{4\omega_{\mathbf{q}}^2} + \mathcal{O} \left( \frac{\Gamma^2}{\omega^2} \right). \quad (\text{B3})$$

As expected, (B3) is recognized to be the usual 1-loop correction to the quartic coupling constant.

For  $n = 1$ , the first order in the adiabatic approximation, which will give the dissipation coefficient, we obtain (again retaining terms up to first order in  $\Gamma$ )

$$\begin{aligned}
& \int_{-\infty}^t dt' (t' - t) \text{Im} \left[ G^{++}(\mathbf{q}, |t-t'|) G^{++}(\mathbf{q}-\mathbf{k}, |t-t'|) \right] \\
& \simeq -[1 + 2n(\omega_{\mathbf{q}})] \frac{3\omega_{\mathbf{q}}^2 + \omega_{\mathbf{q}-\mathbf{k}}^2}{\omega_{\mathbf{q}} (\omega_{\mathbf{q}}^2 - \omega_{\mathbf{q}-\mathbf{k}}^2)^2 (\omega_{\mathbf{q}} - \omega_{\mathbf{q}-\mathbf{k}})} \frac{\Gamma_{\mathbf{q}} + \Gamma_{\mathbf{q}-\mathbf{k}}}{\omega_{\mathbf{q}} + \omega_{\mathbf{q}-\mathbf{k}}} + (\omega_{\mathbf{q}} \rightleftharpoons \omega_{\mathbf{q}-\mathbf{k}}) \\
& -\beta \Gamma_{\mathbf{q}} n(\omega_{\mathbf{q}}) [1 + n(\omega_{\mathbf{q}})] \frac{1}{(\omega_{\mathbf{q}}^2 - \omega_{\mathbf{q}-\mathbf{k}}^2)^2} + (\omega_{\mathbf{q}} \rightleftharpoons \omega_{\mathbf{q}-\mathbf{k}}) + \mathcal{O} \left[ \left( \frac{\Gamma_{\mathbf{q}} + \Gamma_{\mathbf{q}-\mathbf{k}}}{\omega_{\mathbf{q}} + \omega_{\mathbf{q}-\mathbf{k}}} \right)^3 \right]. \quad (\text{B4})
\end{aligned}$$

We can see, in contrast with (B2), that the limit  $\mathbf{k} \rightarrow 0$  is divergent. This divergence is reminiscent of the on-shell singularity which is present in the integral in (B4) when bare propagators are used, thus showing the importance of  $\Gamma$  as a regulator. By first taking the homogeneous limit  $\mathbf{k} \rightarrow 0$  and then expanding in  $\Gamma$ , we obtain the result given in the text, which is the first term on the RHS in (3.5).

The same calculation can be performed for the  $n = 2$  case, the second order in the adiabatic expansion, from which we obtain

$$\lim_{\mathbf{k} \rightarrow 0} \int_{-\infty}^t dt' (t' - t)^2 \text{Im} \left[ G^{++}(\mathbf{q}, |t-t'|) G^{++}(\mathbf{q}-\mathbf{k}, |t-t'|) \right] \rightarrow \frac{1 + 2n(\omega_{\mathbf{q}})}{16\omega_{\mathbf{q}}^5} + \mathcal{O} \left( \frac{\Gamma^2}{\omega^2} \right). \quad (\text{B5})$$

This result is consistent with a recent calculation in Ref. [44], which addresses the time derivative expansion of the effective action, for a given scalar field model. The authors of

[44] also discuss their work in the context of the non-analyticity problem in finite temperature QFT. In fact, we note that the second order term in the adiabatic approximation can be associated with the first order term in the time derivative expansion of the effective action,  $\sim \mathcal{Z}(\varphi)(\partial_t\varphi)^2$  (for a time-dependent, space-homogeneous field configuration).

## REFERENCES

- [1] N. Goldenfeld, *Lectures on Phase Transitions and the Renormalization Group*, Frontiers in Physics, Vol. 85, (Addison-Wesley, 1992).
- [2] M. Gleiser and R. O. Ramos, Phys. Rev. **D50**, 2441 (1994).
- [3] P. Hänggi, P. Talkner and M. Borkovec, Rev. Mod. Phys. **62**, 251 (1990).
- [4] G. W. Ford, M. Kac, and P. Mazur, J. Math. Phys. **6**, 504 (1965); G. W. Ford and M. Kac, J. Stat. Phys. **46**, 803 (1987).
- [5] A. O. Caldeira and A. J. Leggett, Ann. Phys. **149**, 374 (1983).
- [6] A. Berera, Phys. Rev. **D54**, 2519 (1996).
- [7] A. Berera, Phys. Rev. Lett. **75**, 3218 (1995).
- [8] A. Berera and L. Z. Fang, Phys. Rev. Lett. **74**, 1912 (1995).
- [9] A. Berera, Phys. Rev. **D55**, 3346 (1997).
- [10] A. Berera, L. Z. Fang, and G. Hinshaw, Phys. Rev. **D57**, 2207 (1998).
- [11] A. Hosoya and M. Sakagami, Phys. Rev. **D29**, 2228 (1984).
- [12] E. Calzetta and B.L. Hu, Phys. Rev. **D37**, 3536 (1988); Phys. Rev. **D55**, 3536 (1997).
- [13] D. Boyanovsky, H. J. de Vega, R. Holman, D.-S. Lee and A. Singh, Phys. Rev. **D51**, 4419 (1995).
- [14] M. Morikawa, Phys. Rev. **D33**, 3607 (1986).
- [15] C. Greiner and B. Müller, Phys. Rev. **D55**, 1026 (1997).
- [16] M. Yamaguchi and J. Yokoyama, Phys. Rev. **D56**, 4544 (1997).
- [17] L. P. Kadanoff and G. Baym, *Quantum Statistical Mechanics, Green's Functions Methods in Equilibrium and Nonequilibrium Problems* (Addison-Wesley Publ. Co., NY, 1989).

- [18] G. D. Mahan, *Many-particle Physics* (Plenum, NY, 1981).
- [19] A. Hosoya, M. Sakagami and M. Takao, Ann. Phys. **154**, 229 (1984).
- [20] S. Jeon, Phys. Rev. **D47**, 4586 (1993).
- [21] S. Jeon, Phys. Rev. **D52**, 3591 (1995).
- [22] E. Wang, U. Heinz and X. Zhang, Phys. Rev. **D53**, 5978 (1996); E. Wang and U. Heinz, Phys. Rev. **D53**, 899 (1996).
- [23] R. R. Parwani, Phys. Rev. **D45**, 4695 (1992).
- [24] M. Abramowitz and I. Stegun, *Handbook of Mathematical Functions*, Dover Publ., (New York 1972).
- [25] J. Schwinger, Jour. Math. Phys. (N.Y.) **2**, 407 (1961); P. M. Bakshi and K. T. Mahanthappa, Jour. Math. Phys. (N.Y.) **4**, 1 (1963); **4**, 12 (1963); L. V. Keldysh, Zh. Eksp. Teor. Fiz. **47**, 1515 (1964); A. Niemi and G. Semenoff, Ann. Phys. (NY) **152**, 105 (1984); Nucl. Phys. **B230**, 181 (1984).
- [26] K. Chou, Z. Su, B. Hao and L. Yu, Phys. Rep. **118**, 1 (1985).
- [27] An accessible introduction to the real-time formalism can be found in R. Rivers, *Path Integral Methods in Quantum Field Theory*, Cambridge University Press, (Cambridge 1987).
- [28] N. P. Landsman and Ch. G. van Weert, Phys. Rep. **145**, 141 (1987).
- [29] P. Fendley, Phys. Lett. **B196**, 175 (1987).
- [30] M. Gleiser, E. W. Kolb, and R. Watkins, Nucl. Phys. **B364**, 411 (1991); G. Gelmini and M. Gleiser, Nucl. Phys. **B419**, 129 (1994); M. Gleiser and E. W. Kolb, Phys. Rev. Lett. **69**, 1304 (1992); N. Tetradis, Z. Phys. **C57**, 331 (1993).
- [31] M. Gleiser and R. O. Ramos, Phys. Lett. **B300**, 271 (1993).

- [32] K. Kajantie, M. Laine, K. Rummukainen, and M. Shaposhnikov, Nucl. Phys. **B493**, 1 (1997).
- [33] G. Semenoff and N. Weiss, Phys. Rev. **D31**, 699 (1985).
- [34] A. Ringwald, Ann. Phys. **177**, 129 (1987); Phys. Rev. **D36**, 2598 (1987); H. Leutwyler and S. Mallik, Ann. Phys. **205**, 1 (1991).
- [35] M. Dine, R. Leigh, P. Huet, A. Linde and D. Linde, Phys. Rev. **D46**, 550 (1992).
- [36] D. Boyanovsky, R. Holman and S. Prem Kumar, Phys. Rev. **D56**, 1958 (1997).
- [37] J. Ellis and G. Steigman, Phys. Lett. **B89**, 186 (1980).
- [38] K. Enqvist and J. Sirkka, Phys. Lett. **B314**, 298 (1993).
- [39] H. P. de Oliveira and R. O. Ramos, Phys. Rev. **D57**, 741 (1998).
- [40] A. Linde, Phys. Lett. **B129**, 177 (1983).
- [41] G. Mazenko, W. Unruh and R. Wald, Phys. Rev. **D31**, 273 (1985).
- [42] P. D. B. Collins and R. F. Langbeim, Phys. Rev. **D45**, 3429 (1992); **D47**, 2302 (1993).
- [43] D. J. Gross, R. D. Pisarski and L. G. Yaffe, Rev. Mod. Phys. **53**, 43 (1981); H. A. Weldon, Phys. Rev. **D28**, 2007 (1993); *ibid.* **D47**, 594 (1993); T. S. Evans, Can. J. Phys. **71**, 241 (1993); A. Das and M. Hott, Phys. Rev. **D50**, 6655 (1994);
- [44] M. Asprouli and V. G.-Gonzalez, hep-ph/9802319.

## FIGURE CAPTIONS

**Figure 1:**  $\text{Im}\Sigma_\chi(\mathbf{q}, \omega_\chi(\mathbf{q}))$  normalized by its  $|\mathbf{q}| = 0$  value, for different values of masses and space momentum.

**Figure 2:** The dissipation coefficient  $\eta_1$  computed (for  $N = 25$ ) with  $\text{Im}\Sigma_\chi(\mathbf{q}, \omega_\chi(\mathbf{q}))$  and with the approximation  $|\mathbf{q}| = 0$  for the imaginary part of the self-energy.

**Figure 3:** Results for the adiabatic condition, Eq. (4.7). The dashed lines correspond to  $|\dot{\varphi}_c/\varphi_c|$ , for different values for  $\varphi_c$ . The solid line corresponds to  $\Gamma_\chi(q)$ , evaluated at  $|\mathbf{q}| = T$ . All cases shown are for  $N = 25$ . The region satisfying the adiabatic condition is the intersection of the region above the dashed lines with the region below the solid line. Fig. 3a is for  $\lambda = g^2$ , Fig. 3b is for  $\lambda = g$  and Fig. 3c is for  $\lambda_T = g^4$ .

FIGURES

Figure 1

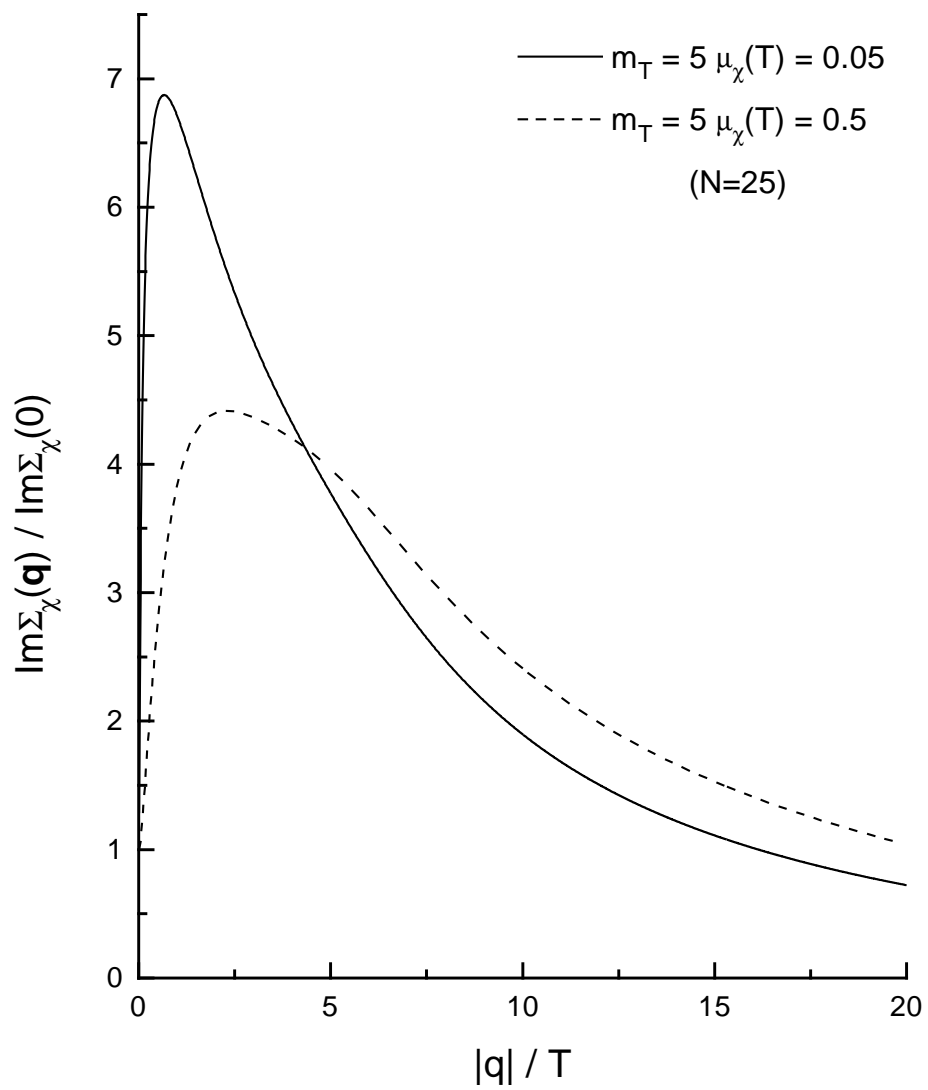




Figure 2

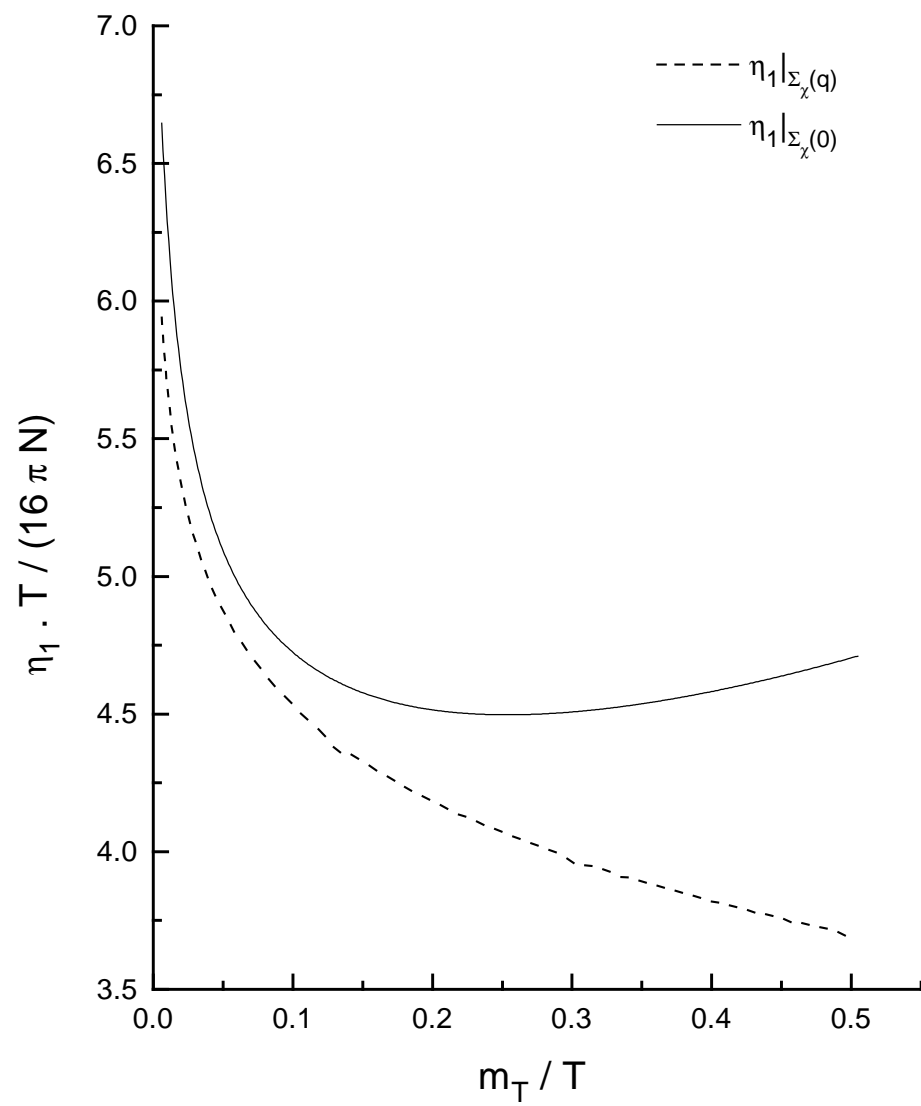


Figure 3a

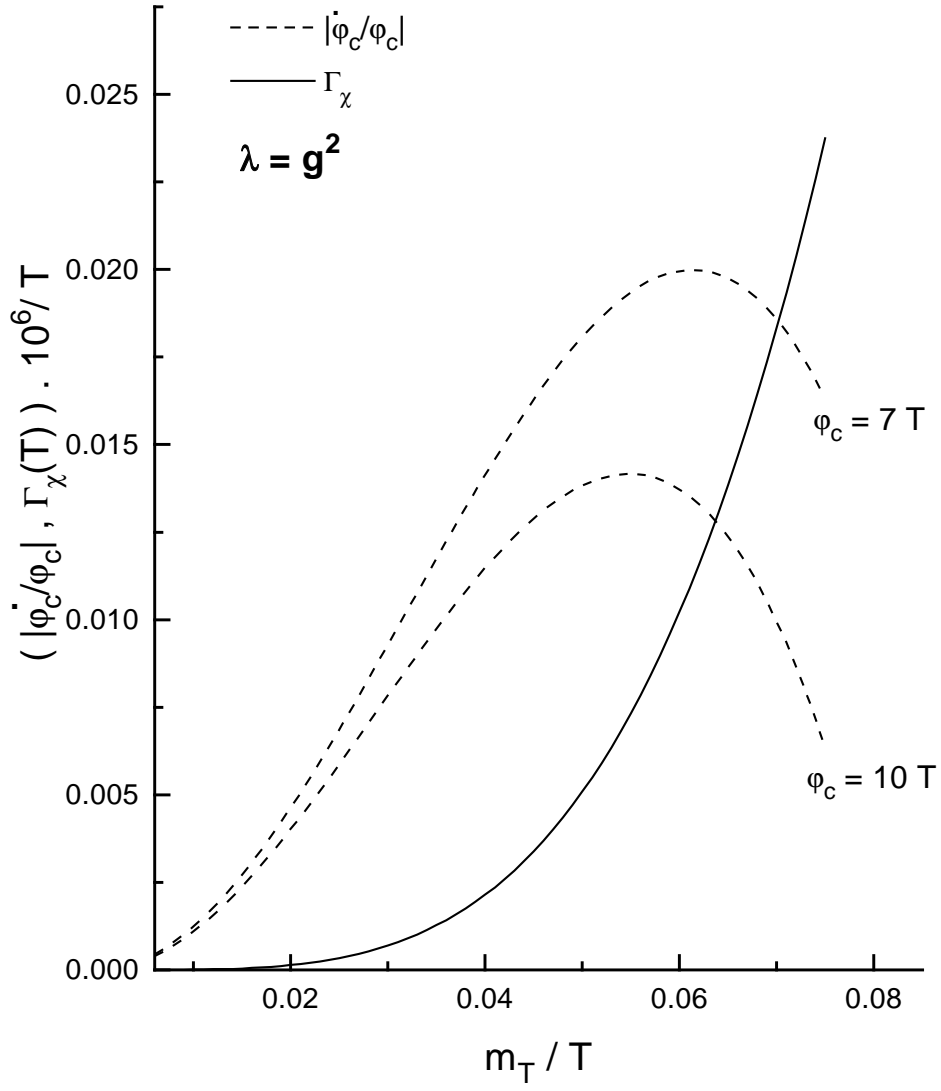


Figure 3b

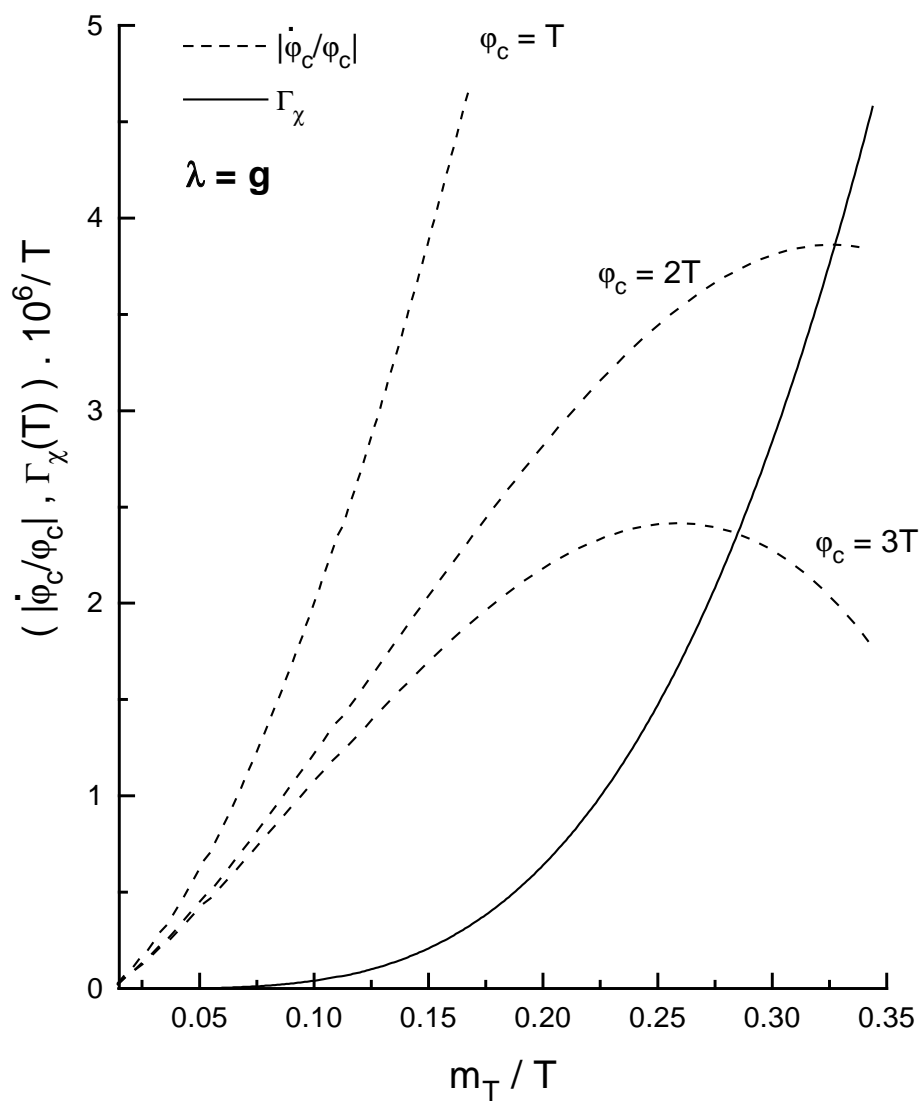


Figure 3c

